CIRCULATION COPY
SUBJECT TO RECALL
IN TWO WEEKS

UCRL-84230-R-1
PREPRINT

GEOLOGICAL, GEOPHYSICAL, AND THERMAL CHARACTERISTICS OF THE SALTON SEA GEOTHERMAL FIELD, CALIFORNIA

L. W. Younker
P. W. Kasameyer
J. D. Tewhey

This paper was prepared for submittal to the
Journal of Volcanology and Geothermal Research.

June 18, 1981

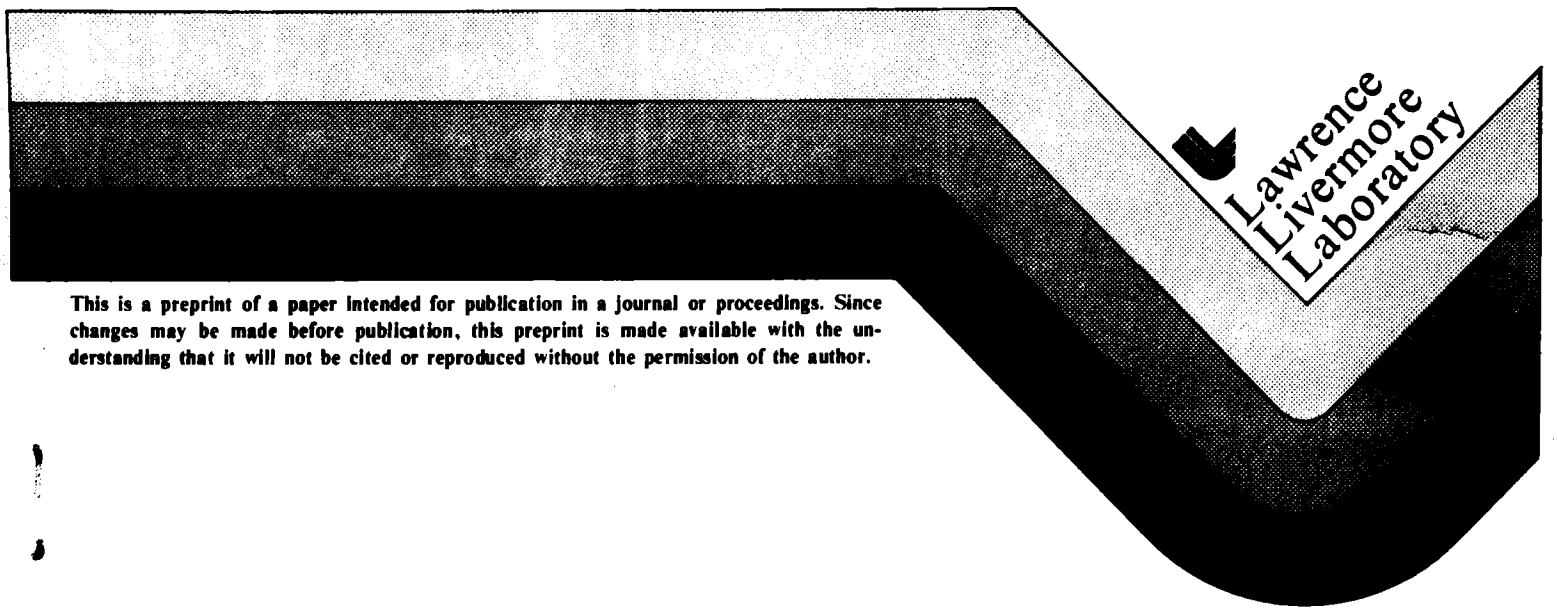

This is a preprint of a paper intended for publication in a journal or proceedings. Since changes may be made before publication, this preprint is made available with the understanding that it will not be cited or reproduced without the permission of the author.

DISCLAIMER

This document was prepared as an account of work sponsored by an agency of the United States Government. Neither the United States Government nor the University of California nor any of their employees, makes any warranty, express or implied, or assumes any legal liability or responsibility for the accuracy, completeness, or usefulness of any information, apparatus, product, or process disclosed, or represents that its use would not infringe privately owned rights. Reference herein to any specific commercial products, process, or service by trade name, trademark, manufacturer, or otherwise, does not necessarily constitute or imply its endorsement recommendation, or favoring of the United States Government or the University of California. The views and opinions of authors expressed herein do not necessarily state or reflect those of the United States Government or the University of California, and shall not be used for advertising or product endorsement purposes.

GEOLOGICAL, GEOPHYSICAL, AND THERMAL CHARACTERISTICS OF THE SALTON SEA GEOTHERMAL FIELD, CALIFORNIA

LELAND W. YOUNKER, PAUL W. KASAMEYER and JOHN D. TEWHEY

Earth Sciences Division, University of California, Lawrence Livermore National Laboratory, Livermore, CA 94550 (U.S.A.)

ABSTRACT

Younker, L.W., Kasameyer, P.W. and Tewhey, J.D., 1981. Geological, geophysical, and thermal characteristics of the Salton Sea Geothermal Field, California. J. Volcanol. Geotherm. Res., .

The Salton Sea Geothermal Field is the largest water-dominated geothermal field in the Salton Trough in Southern California. Within the trough, local zones of extension among active right-stepping right-lateral strike-slip faults allow mantle-derived magmas to intrude the sedimentary sequence. The intrusions serves as heat sources to drive hydrothermal systems.

We can characterize the field in detail because we have an extensive geological and geophysical data base. The sediments are relatively undeformed and can be divided into three categories as a function of depth: (1) low-permeability cap rock, (2) upper reservoir rocks consisting of sandstones, siltstones, and shales that were subject to minor alterations, and (3) lower reservoir rocks that were extensively altered. Because of the alteration,

intergranular porosity and permeability are reduced with depth. Field permeability is enhanced by renewable fractures, i.e., fractures that can be reactivated by faulting or natural hydraulic fracturing subsequent to being sealed by mineral deposition.

In the central portion of the field, temperature gradients are high near the surface and lower below 700 m. Surface gradients in this elliptically shaped region are fairly constant and define a thermal cap, which does not neccessarily correspond to the lithologic cap. At the margin of the field, a narrow transition region, with a low near-surface gradient and an increasing gradient at greater depths, separates the high temperature resource from areas of normal regional gradient. Geophysical and geochemical evidence suggest that vertical convective motion in the reservoir beneath the thermal cap is confined to small units, and small-scale convection is superimposed on large-scale lateral flow of pore fluid.

Interpretation of magnetic, resistivity, and gravity anomalies help to establish the relationship between the inferred heat source, the hydrothermal system, and the observed alteration patterns. A simple hydrothermal model is supported by interpreting the combined geological, geophysical, and thermal data. In the model, heat is transfered from an area of intrusion by lateral spreading of hot water in a reservoir beneath an impermeable cap rock.

INTRODUCTION

The Salton Sea Geothermal Field is one of several water-dominated geothermal fields in the Salton Trough, a sediment-filled rift valley that represents the landward extension of the Gulf of California into North America. The area has been the subject of intensive geologic investigation

for several reasons. It is a seismically active region and a significant link in the transition from the divergent plate boundary of the East Pacific Rise to the transform boundary of the San Andreas fault system (Elders et al., 1972; Lomnitz et al., 1970; Elders and Biehler, 1975). Hot brines are present at depth in the field making the area ideally suited for the study of active hydrothermal alteration and ore deposition (Helgeson, 1968; Muffler and White, 1969; Skinner et al., 1967). Finally from a more applied viewpoint, it is one of the largest and most accessible geothermal resource areas in North America (Towse, 1975; Renner et al., 1975; Nathenson and Muffler, 1975; Biehler and Lee, 1977; Younker and Kasameyer, 1978). With detailed understanding, this region can be exploited efficiently.

Our purpose is to characterize the thermal anomaly and show its relationship to the geological and geophysical features of the field. In the first section we review the geological characteristics of the field. This description is based largely on information from logs of 16 geothermal wells and from drill cuttings and core samples from 3 wells (Tewhey, 1977). The information is broadly consistent with other recent descriptions of the field (McDowell and Elders, 1979). In the second section we briefly review the geophysical characteristics of the field, with emphasis on aspects relating to the nature of the heat source. In the final section we analyze in detail the subsurface temperatures and the surface gradient data to infer the mechanisms of heat transfer throughout the system. We then summarize the information from these three sets of observations and arrive at an overview of the geothermal system. In a future paper we will present a quantitative heat-transfer model consistent with these characteristics and the overall tectonic setting.

THE GEOLOGIC CHARACTERISTICS OF THE SALTON SEA GEOTHERMAL FIELD

Geologic setting

The Salton Trough is the northern portion of a structural and topographic basin extending from southern California to the southern end of the Gulf of California. From its origin in the Miocene (Dibblee, 1954; Hamilton, 1961) until mid-Pleistocene (Downs and Woodward, 1961), the trough received sediments from the Colorado River. In mid-Pleistocene, possibly during a period when the sea level was low, the Colorado River delta was built westward across the trough from Yuma, Arizona. Deltaic sediments accumulated during this time and the northern portion of the basin, i.e., the Salton Trough, was topographically separated from the Gulf of California. The Salton Sea represents the latest in a long sequence of inland seas that have occupied the trough since the Pleistocene (Van De Kamp, 1973).

Geological (Dibblee, 1954) and geophysical evidence (Biehler et al., 1964) shows that the sequence of sedimentary rocks in the Salton Trough is approximately 6000 m thick. Based on results of field work in the folded sedimentary rocks along the margins of the trough and examination of cuttings from the 4097-m Wilson No. 1 well near Brawley, the 6000-m sequence is composed largely of detritus from the Colorado River. Only minor contributions appear to have come from the Chocolate Mountains and Peninsular ranges bordering the trough on the east and west (Muffler and White, 1969). The unaltered deltaic sediments in the Salton Trough have a rather uniform composition consisting predominantly of quartz and calcite and subordinately of dolomite, feldspar, clay minerals, mica, and accessory minerals.

The present description of reservoir geology is based on information in logs from 16 geothermal wells and drill cutting and core samples from 3 wells (Tewhey, 1977). The wells from which samples were obtained are located in the west-central portion of the Salton Sea Geothermal Field, i.e., Magmamax Nos. 2 and 3 and Woolsey No. 1 (Fig. 1). The three wells are 1331, 1219, and 1064 m deep, respectively. The cutting samples were examined microscopically and specific samples were selected for petrographic, x-ray diffraction, and microprobe analyses. The petrographic analyses and porosity measurements were done on core samples. The drill cutting samples yielded evidence of a sedimentary sequence in the study area from the surface to below 1300 m that can be divided into three categories: (1) cap rock, (2) upper, slightly altered, reservoir rocks, and (3) lower, extensively altered, reservoir rocks. This is shown in Fig. 2.

Sedimentary sequence

The cap rock

The cap rock of a geothermal system is the thick layer of low permeability rock that overlies the more permeable reservoir rocks. It can serve both as a barrier for circulating convection currents and as a thermal insulator, thereby contributing to the increase in temperature in the geothermal system.

In the Salton Sea Geothermal Field, the cap rock thickness is variable and, generally,is thickest (~700 m) in the northern portion of the field and thinnest (~250 m) in the southern portion (Randall, 1974). Based on analysis of geophysical data from logs and observation of cutting samples near

the Magmamax wells, the cap rock is 340 to 370 m thick (Fig. 2). Two distinct layers are present in the cap. The material in the upper 200 m consists of unconsolidated clay, silt, sand, and gravel. The material from 200 m to the bottom of the cap rock sequence consists primarily of anhydrite-rich evaporite layers, often in a carbonate matrix. The evaporite layers are consolidated and not friable, and the interlocking textures of anhydrite and carbonate grains indicate low permeability. Gypsum commonly precipitates from sea water. However, its stability field is limited to environments near the surface, because during burial and diagenesis, gypsum is dehydrated and converted to anhydrite (Berner, 1971). The relatively thick sequence of evaporite-rich deposits that make up the cap rock are indicative of the long sequence of intermittent Salton Seas that existed in the basin since its isolation from the Gulf of California.

Facca and Tonani (1967) have shown empirically that hot water circulating in a hydrothermal system can produce alteration and deposition along flow paths in the cap rock and, thereby, reduce permeability. In this manner, a geothermal system can be self-sealing by producing or restoring its own cap rock. Direct evidence of the self-sealing phenomenon was provided by Batzle and Simmons (1976), who examined samples of cap rock from the Dunes area of the Salton Trough using the scanning electron microscope. They interpreted minute veinlets and fluid inclusion trains as microcracks that were healed by minerals precipitating from circulating fluids. There is evidence to suggest that crack production and subsequent sealing are not limited to the cap rock but occur in reservoir rocks at the Salton Sea field as well. This will be discussed in a later section.

Upper reservoir rock

Technically, there are no unaltered sediments in the cuttings examined for this study. Thermal springs at the surface indicate that hot brines penetrated and permeated the entire sedimentary section. The effects of brine-induced alterations in the uppermost reservoir rocks are principally silicification and clay mineral reactions. An example of the latter is that kaolinite and montmorillonite are transformed to chlorite or illite (Muffler and White, 1969).

With the exception of pyrite mineralization, the rock alteration above 800 m in the Magmamax wells and above 1000 m in the Woolsey well is detectable only by means of careful x-ray diffraction analysis or detailed petrographic studies. These secondary alterations did not result in marked changes in the petrophysical properties (e.g., porosity and permeability) of the reservoir rocks.

The sharp transition between reservoir rocks and the overlying cap rock is interpreted as representing the boundary between marine sediments (reservoir rock) deposited in the Gulf of California and lacustrine sediments (cap rock) deposited in the Salton Trough after it was isolated from the southern portion of the basin in the mid-Pleistocene. Dibblee (1954) and Dutcher et al. (1972) consider the entire Miocene-Pleistocene section in the Salton Trough as a conformable sequence.

In the Magmamax Nos. 2 and 3 wells, the zone of slightly altered reservoir rocks is approximately 480 m thick, extending from a depth of 340 m to nearly 820 m. In Woolsey No. 1, the zone is 660 m thick, from 340 to 1000 m. The thickness of this zone increases to the east and, to a lesser extent, to the

north and is related to the heat distribution in the geothermal field. The slightly altered sequence in the Magmamax and Woolsey wells consists of indurated sandstones, siltstones, shales, and a few thin coal seams. The sandstone contains subangular clastic grains of quartz with minor feldspar, mica, chlorite, and lithic fragments. The rocks exhibit varying degrees of calcite cementation and intergranular porosity ranging from 10 to 30%.

The first appearance of epidote in reservoir rocks is used to mark the transition to high-rank alteration. The epidote producing reaction is temperature dependent and corresponds approximately to the present-day 280°C isotherm.

Hydrothermally altered reservoir rocks

The mineralogical and textural changes in deep-seated rocks in the Salton Sea Geothermal Field can be attributed to hydrothermal alteration in an open system with a large mass-transfer of chemical constituents. The important variables seem to have been permeability, temperature, brine composition, and original rock composition. At the temperatures characteristic of the Magmamax wells ($\leq$ 300°C), sandstones, and siltstones were appreciably altered, but the less permeable shales were relatively little affected. Heat-induced metamorphism occurs in shales in the deeper portions of the reservoir.

The hydrothermally altered deltaic sediments that constitute the reservoir rocks can be described chemically by the complex system K_2O-Na_2O-CaO-MgO-FeO-Fe_2O_3-Al_2O_3-SiO_2-CO_2-H_2O-S. To interpret the observed mineral assemblages, as well as those that might be encountered at depth, it is necessary to reduce the complex system to the simple well-studied

subsystem of $CaO-Al_2O_3-SiO_2-CO_2-H_2O$. The isobaric phase relations at 2 kb in the subsystem as a function of temperature and mole fraction CO_2 are depicted in Fig. 3.

Calcite is a principal component of upper, slightly altered, reservoir rocks and epidote is common in the lower rocks. The gradual disappearance of calcite with depth coincides with the development of epidote as an alteration product. The mineralogical observations and the presence of abundant CO_2 at shallow depths in the geothermal field can be accounted for by the evolution of CO_2 through the reaction,

calcite + 3 anorthite (plagioclase feldspar) + water $\rightleftharpoons$ 2 zoisite (Fe-free epidote) + carbon dioxide.

The slope of the univariant line representing this reaction (Fig. 3) is near infinity, thus, the sign of dT/dX_{CO_2} is difficult to determine experimentally. If dT/dX_{CO_2} is positive, the transition from calcite to zoisite (epidote) will occur as the temperature increases. If the sign of dT/dX_{CO_2} is negative, the calcite to zoisite transition will be largely pressure dependent. Therefore, if the sign of dT/dX_{CO_2} is either positive or negative, a mechanism exists for the transition of epidote to calcite as the depth increases.

Grossularite-andradite garnet has been found in cuttings from the deepest wells in the Salton Sea field (Kendall, 1976; McDowell and McCurry, 1977); therefore, the reaction path shown in Fig. 3 can be extended into the garnet field by the reaction

4 zoisite (Fe-free epidote) + quartz $\rightleftharpoons$ grossularite (garnet) + 5 anorthite + 2 water.

The nature of the transition from slightly altered to more extensively altered rocks in the Salton Sea field was determined by petrographic, x-ray

diffraction, and election microprobe analyses. Both the chemical (mineralogical) and physical changes that result from alteration were studied. Epidote is first seen at 811 m in Magmamax 2, at 826 m in Magmamax 3 and at 1006 m in Woolsey 1. Muffler and White (1969) report first seeing epidote at 1052 m in IID No. 1 well and 1167 m in Sportsman No. 1 well. Although the data base is scanty, the contours of the epidote isograd, i.e., the first appearance of epidote, are concentric with the heat axis as defined by Randall (1974) and the pattern of subsurface isotherms as determined by Palmer (1975).

High-rank hydrothermal alteration of the reservoir rocks in the Salton Sea Geothermal Field has reduced porosity and permeability. Epidote and silica are the principal pore filling minerals produced during high temperature alteration. They replace calcite and anhydrite, the cementing agents produced during diagenesis. The process of the self-sealing geothermal field (Facca and Tonani, 1967), discussed earlier, is beneficial when it creates an impermeable cap rock over a shallow geothermal reservoir, but it can be detrimental when it reduces porosity and permeability in reservoir rocks.

Porosity was determined on core samples from geothermal wells at the Salton Sea (see Fig. 4), and a reduction of porosity was noted with depth. This is common in sedimentary basins and is enhanced in the Salton Sea Geothermal Field by hydrothermal alteration.

In the area studied, data from geophysical logs and drill cores indicate that the reservoir strata dip westward toward the center of the geothermal resource at approximately 10 degrees. In the presence of the vertical porosity gradient, the dipping strata become less porous and less permeable from the periphery of the field toward the center of the heat axis (Fig. 2).

Significance of fracture porosity and permeability

Fractures provide a substantial portion of the permeability and reservoir capacity in a number of geothermal fields, e.g., Geysers, Otake, Larderello, Wairakai, and Broadlands (Facca, 1973). The primary intergranular porosity in a reservoir is subject to irreversible self-sealing; however, fractures can be considered to have renewable porosity, or permeability, or both, because they can be reactivated after being filled or sealed. The fracture producing mechanism may be either faulting (many major geothermal fields are located in areas with active tensional tectonics) or natural hydraulic fracturing resulting from high fluid pressures in the reservoir (Grindley and Browne, 1976).

The hydrothermally altered reservoir rocks in the Salton Sea Geothermal Field are extensively fractured, especially the shales. Fracture widths range from a few micrometres to 1 mm. The location of the Salton Sea field on an active spreading zone (Elders et al., 1972) ostensibly can account for the many fractures in the reservoir.

Evidence for the renewability of fracture porosity and permeability after sealing is found in the form of (1) calcite filled veins in which the calcite was mechanically twinned and deformed after deposition, indicating there was renewed stress on an old fracture; (2) calcite filled veins reactivated (refractured) and then refilled with epidote; and (3) anhydrite veins that reveal two or more episodes of fracturing and deposition when viewed with cathodoluminescence (see Fig. 5). These observations suggest that the seismic activity in the Salton Trough may maintain fracture permeability in the reservoir.

Subsurface structure

Subsurface sedimentary strata were correlated among 10 geothermal wells in the Salton Sea field. Two cross sections were constructed. The north to south section extends for 4 km from the Elmore No. 1 well in the northern to the Sinclair No. 3 well in the southern portion of the field (Fig. 6). An east to west section extends for 2 km in the central portion of the field and encompasses the Magmamax and Woolsey wells (Fig. 2). The spontaneous potential (SP) log, the principal tool used for correlation purposes, is useful to detect permeable sandstones, determine qualitative indications of bed shaliness, and locate boundaries between sand and shale units.

The evaporite and carbonate-rich cap rock sequence (most of which is not seen in Fig. 6) produces a flat, featureless SP curve of little use for detailed correlation. The potential for correlation is also somewhat reduced in the zone of hydrothermally altered reservoir rock. Hydrothermal alteration promotes the growth of new minerals in the pore space of permeable sandstones and in shale partings and fractures. The alteration limits the response of diverse rock types to the SP log that, in turn, makes correlating more difficult.

The structural picture emerging from these and other cross sections is one of a broad syncline with an east to west axis approximately perpendicular to the axis of the Salton Trough. The syncline has a shallow westward plunge toward the center of the trough, and there is a general tendency for north to south thickening of individual sedimentary units.

Igneous Activity

The Salton Sea Geothermal Field has five rhyolite buttes arranged along a northeast trend at the southern end of the sea. These buttes are spaced 3 to 4 km apart, and were extruded over Quaternary alluvium. Robinson et al. (1976) noted that these rhyolites were similar in composition to those on islands of the East Pacific Rise and that basaltic inclusions within the rhyolites from the Salton Sea buttes are similar to the low-potassium tholeiitic basalts from the rise. This bimodal rhyolite plus basalt association is a common feature of regions characterized by tensional tectonics. Evidence suggesting subsurface igneous activity in the region includes the gravity and magnetic anomalies discussed below and the presence of altered basaltic and silicic dikes and sills in several of the geothermal wells at a depth of 1 to 2 km (Robinson et al., 1976).

GEOPHYSICAL CHARACTERISTICS OF THE SALTON SEA GEOTHERMAL FIELD

Tectonic setting

The Salton Sea Geothermal Field is a significant link in the transition from the divergent plate boundary of the East Pacific Rise to the transform boundary of the San Andreas fault system. North of the Salton Sea, and within the Salton Trough, the right lateral San Andreas fault system consists of three subparallel strands, i.e., the Banning-Mission Creek, the San Jacinto, and the Elsinore. South of the Salton Sea, these strands lose their character

and merge into a series of smaller, less distinct, subparallel faults. Based on recent seismicity within the Imperial Valley, the most important faults are the side-stepping Imperial, Brawley, and Calipatria (Fig. 1).

Lomitz et al. (1970) noted that the spreading centers in the Gulf of California are offset by right-stepping en echelon faults, in a manner similar to that displayed in the Imperial Valley on a smaller scale. They suggested that the tectonic framework in the northern portion of the Gulf of California and the Salton Trough could be understood by considering these strike-slip faults as transform faults connected by short spreading centers. Within the Salton Trough, they postulated, active ridge segments account for the geothermal anomalies near Cerro Prieto and the Salton Buttes. Elders et al. (1972) expanded and refined the model using geophysical, petrological, and geodetic data from the trough. They suggested active speading centers occur in tensional gaps between en echelon strike-slip faults. Elders and Biehler (1975) and Hill et al. (1975) label these areas leaky transform faults; the dominant movement in the region is strike slip, with spreading taking place in a rather diffuse zone of offset strike-slip faults. The complex interaction of extensional and strike-slip movement is responsible for the overall structure of the trough.

The general model of crustal rift formation by leaky transform faulting is supported by gravity, seismic, and leveling data. A gravity maximum in the center of the trough can be explained by 8 km of crustal thinning (Biehler, 1971). Fuis et al. (1980) used over 3000 seismograms from 1300 stations and found a high velocity crust at depths of 10 to 16 km under two thirds of the Imperial Valley. They interpret this region as having an oceanic-type crust

that formed from the intrusion of mantle-derived materials into areas of extension. Vertical leveling data collected since 1900 indicate ongoing deepening of the Salton Trough consistent with the general model of rifting (Lofgren, 1978).

Seismicity in the Salton Trough is characterized by both large earthquakes and swarms of small-magnitude earthquakes (Hill et al., 1975; Sylvester, 1979; Johnson, 1979). The large earthquakes obviously result from the relative motion between the North American and Pacific plates; however, the swarm activity has been related to hydraulic fracturing (Johnson, 1979) or magmatic processes (Hill, 1977). The relationship between the swarm events and the major events has not been established, but the general pattern of seismicity, as revealed in epicenter locations and first motion studies, is consistent with the combination of regional shearing and local extension required by the leaky transform model (Weaver and Hill, 1978).

The Salton Sea Geothermal Field is one of the thermal anomalies within the Salton Trough, where the active processes associated with crustal thinning and rifting can be directly observed. A wide range of geophysical surveys near the Salton Sea helped to detail critical aspects of the hydrothermal system.

Geophysical anomalies associated with the field

Gravity, magnetic and resistivity surveys show many features of the Salton Sea Geothermal Field (Figs. 7-9). A local gravity maximum within the geothermal area is approximately centered on Red Island Rhyolite butte (Fig. 7). Elders et al. (1972) attributed the local anomaly to either an

increase in density of the sediments resulting from hydrothermal alteration, or the intrusion of dikes and sills into the sedimentary section, or both.

The magnetic surveys of Griscom and Muffler (1971) and Kelley and Soske (1936) reveal the presence of material with a relatively high susceptibility and remanent magnetization near the surface (Fig. 8). Griscom and Muffler separated the major anomaly into three superimposed ones, with the dominant feature a magnetic ridge trending northwest from Calipatria to the middle of the Salton Sea. Two elliptical northeast-trending anomalies are superimposed upon the ridge; and small intense anomalies clearly associated with the volcanic domes are, in turn, superimposed on the elliptical anomalies. They interpreted the magnetic ridge to be caused by intrusive rocks at depths greater than 2 km and the elliptical anomalies to be a result of dike and sill clusters at depths of approximately 1 km beneath the surface.

Meidav et al. (1976) made a recent resistivity survey in the vicinity of the geothermal field. Electrical currents as high as 200 A were used to detect resistivities of less than 0.5 Ω to depths of several kilometres. The survey consisted of 60 soundings with maximum separation of over 5 km and approximately 60 km of dipole survey lines. In these soundings, the deepest layer they could detect was almost always resistive. The total transverse conductance of the overlying layers was calculated from each sounding curve using the method described by Kell and Frischknecht (1966). The conductance value, essentially the sum of the products of conductivity thickness for all the overlying layers, is the most accurately determined quantity for resistivity soundings. A contour map of the conductance determined from the data of Meidav et al. (1976) is seen in Fig. 9. A large volume of the

sedimentary rock, located between the surface and 2 km, is seen as highly conductive. The conductivity and thickness product (conductance) of this sedimentary sequence is greatest in the area of the drilled field, but a broad area of high conductance extends along the axis of the valley (Kasameyer, 1976).

Low resistivity zones result when porous rocks are saturated with fluid that is hot or saline, or both. Thus the physical boundaries of a porous geothermal reservoir of saline fluid may be determined from resistivity data. In the center of the Salton Sea Geothermal Field, the low resistivity results presumably from both increased temperature and salinity. The resistivity increases rapidly to the northeast and southwest of the known field, indicating a loss of porosity or lower temperature and salinity of the fluid. An area of low resistivity extends southeast from the known geothermal area, and extremely low resistivities (0.5 Ω-m) were detected in the vicinity of a relatively cool well located 6 km from the Salton Sea Geothermal Field. The low resistivity here is inferred to be the result of saline fluid in high porosity rock.

Seismic refraction survey

A large-scale survey of the field involving seven seismic refraction profiles and four long-distance refraction shots was recently completed (Frith 1978). One interpretation of data from a seismic profile that crosses the Salton Sea Geothermal Field is shown in Fig. 10. The location of the profile is seen on the gravity anomaly map (Fig. 7).

If this profile is compared with others in the Imperial Valley, an anomalously high velocity at shallow depths within the Salton Sea Geothermal Field can be seen. Combs and Hadley (1977) reported a velocity of 2.60 km/s at a depth of 0.9 km for an area near the East Mesa geothermal anomaly, and Biehler et al. (1964) a velocity of 2.71 km/s at a similar depth near Westmorland. The higher velocity of 4.06 km/s in the Salton Sea field at comparable depths probably results from intrusion of basaltic material near the surface or the reduction of sediment porosity with hydrothermal alteration.

Seismicity and inferred faults

The Salton Sea field is located in the offset region between the San Andreas fault and the Brawley fault. As a result, the region is subject to intensive seismic activity (Fig. 11) (Schnapp and Fuis, 1977). Faults were identified by geophysical and geological techniques, and their locations in the geothermal field are shown in Fig. 1. The Brawley fault zone was identified by a portable seismic survey (Gilpin and Lee, 1978) and a resistivity survey (Meidav and Furgerson, 1972). The Calipatria fault was identified using infrared detection (Babcock, 1971) and the alignment of thermal hot springs (Muffler and White, 1968). The Red Hill fault, located between the Brawley and the Calipatria faults, was traced with correlations derived from electric logs (Towse, 1975), interpreted from the ground magnetic survey (Meidav and Furgerson 1972), and subsequently located with a seismic refraction survey (Frith 1978).

THERMAL CHARACTERISTICS OF THE SALTON SEA GEOTHERMAL FIELD

Subsurface temperature data

Temperature data from the deep wells in the Salton Sea Geothermal Field (Helgeson, 1968; Randall, 1974; Palmer, 1975; Magma Power Co., 1979) were critically analyzed to determine in which surveys the measurements represent equilibrium temperatures that existed prior to drilling. The data in those surveys were used to gain insight into both the heat source distribution, and the mechanisms of heat transfer within the geothermal field.

The equilibrium profiles for 13 wells within the field are shown in Fig. 12, and two prominent features are evident. First, the field temperatures are high in the lower portions of the profiles. At 2 km they are typically over 320°C, i.e., 200°C higher than at a similar depth in the Wilson No. 1 well, which is 15 km to the south of the field and in a nongeothermal area. Also, temperatures are 140°C higher than those reported in other geothermal fields within the valley. Second, the thermal gradient in the upper part of most of the wells does not change with depth. We can infer from this the general character of the temperature versus depth curve at any location and understand the control of heat transfer within the geothermal system.

Surface gradient analysis for deep wells

The equilibrium temperature profiles discussed above were used to estimate the average gradient in the near-surface conductive zone and the depth to

which the gradient is nearly constant. For wells with enough data, the near-surface temperature measurements were fitted with a straight line. Additional data points from greater depths were added until the fit failed a chi-square test (see Table 1). Surface gradients for wells with few data points were estimated by eye. In all cases the average annual surface temperature was assumed to be 23 $\pm$ 1.0°C. The uncertainty for a single temperature measurement is assumed to be $\pm$ 5°C (one standard deviation, σ) unless stated otherwise.

Nine wells have thermal gradients with similar characteristics and configurations. The gradients are high in the upper portions of the wells (0.38°C/m, 1σ = 0.05°C/m) and are low and nearly constant at greater depths. The transition in the character of the gradient occurs in reservoir rocks beneath the impermeable cap.

Four wells have thermal profiles significantly different from the profiles described above. In Magmamax No. 4, the high gradient at the surface increases slightly (but significantly) with depth in the impermeable cap. In River Ranch No. 1, three measurements in the impermeable cap provide data to suggest a gradual decrease in gradient with depth. However, nearby shallow temperature holes (Lee and Cohen, 1977) indicate a very high local gradient. The proximity of this well to active mud volcanoes and the shallow CO_2 field suggests that the geotherm here is strongly distorted by shallow fluid flow. In the two Sinclair wells, the near surface gradient is low and constant and increases with depth below the impermeable cap.

The general mechanism of heat transport within the lithologic cap can be inferred from these observations. If we assume that thermal conductivity in the cap is uniform in the area determined by the nine wells with similar

profiles, the vertically-conducted heat flow within the lithologic cap is nearly uniform and the horizontally-conducted heat flow negligible. There is no evidence of convective heat flow in the lithologic cap (except near River Ranch No. 1). Furthermore, near these nine wells the thermal boundary conditions on the lithologic cap must have been constant for a sufficiently long time to enable the conductive heat-flow to equilibrate to steady state over a large area and to a great depth.

Because steady state conduction is the dominating heat transfer mechanism in the lithologic cap, we can use shallow thermal holes to determine the gradient of the thermal profile throughout the lithologic cap where deep wells do not exist.

If the subsurface temperature data are compared with the surface gradient analyses, it is possible to arrive at a composite picture of the thermal anomaly. At any location, the temperature versus depth profile down to 2000 m can be described as one of the following:

(A) A nearly constant conductive vertical heat flow in the upper few hundred metres and a nearly isothermal zone at depth. The surface gradient is moderately high, around 0.4°C/m.

(B) Nearly constant heat flow with a value consistent with the normal regional gradient. In these areas the surface gradient is much lower, around 0.1°C/m.

(C) An intermediate region with a low near-surface gradient and an increasing temperature gradient at greater depths.

The distribution of wells based on the descriptions above, is shown in Fig. 13. The data available for shallow wells do not enable us to distinguish

descriptions B and C. Therefore, all shallow wells are labeled either a or b. Those with observed gradients greater than 0.35°C/m are labeled a and those less than 0.16°C/m, b.

Interpreted boundaries define regions containing wells with temperature profiles of similar character. The region with wells labeled A (uniform, moderately high gradient) is elliptical and covers most of the Salton Sea Geothermal Field. Its major axis strikes across the axis of the Salton Trough and is 8 to 12 km in length. The length of the minor axis is unknown because there are no measurements in the Salton Sea. The region containing wells labeled C (transition) includes only the two deep Sinclair wells but is assumed to surround the first region, A. The region with wells labeled B lies outside the others.

The near surface gradient can be used to infer the boundaries of the area of high heat flow. However, the gradient cannot be used successfully to predict temperature differences at depth within the field (see Fig. 14). To predict the temperature at depth, we must determine variations in thickness of the steady-state conduction zone. The thermal profiles from deep wells were also analyzed to determine what geologic factors control this thickness and to predict the temperature at depth in areas where there are no deep wells.

Vertical heat transport

The temperature gradient in wells within the central portion of the anomaly is dramatically reduced at a depth of approximately 500 m, and this is presumed to mark a change in the major mode of heat transport. The upper region is characterized by steep gradients and heat flow by conduction and the

lower by low gradients that, however, must have been supplying heat to the cap long enough for steady state conduction to develop. The dominant heat transfer mechanism in the lower region must be convective flow of pore fluids. We refer to this region as the convective zone.

Previous authors (Dutcher et al., 1972; White, 1968) suggested that vertical heat transport in the Salton Sea field is by large-scale convection cells encompassing the entire section of permeable reservoir rocks. We propose a method to determine the thickness of the zone where conductive heat flow dominates and use it to show that the zone includes a portion of the uppermost section of reservoir rocks immediately beneath the cap rock. Our results suggest the existence of a thermal cap in the Salton Sea field that is thicker in some places than the impermeable lithologic cap described earlier. In addition, we find evidence indicating that thin shale beds impede vertical fluid flow and the amount of convective heat transport in a section is controlled primarily by the thickness of sand beds. Consequently, large-scale vertical convection of fluid cannot take place within that part of the reservoir penetrated by wells.

If most of the heat in the thermal cap is transported by steady state conduction, the heat flow, Q_{cond}, is constant, and the temperature gradient ($\Delta T/\Delta Z$) should vary in the cap inversely with the thermal conductivity of the material, κ, i.e.,

$$Q_{cond} = \kappa \frac{\Delta T}{\Delta Z} = \text{constant} . \qquad (1)$$

If we determine how deep in the reservoir this relationship holds, we can define the lower boundary of the thermal cap.

The relative conductive heat flow at any depth is estimated using the following simplifying assumptions: (1) The lithology consists of infinite horizontal slabs of either pure sandstone or pure shale, as deduced from the electric logs. The analysis does not correct the gradient in the lower lithologic cap for the presence of the anhydrite rich layers. Although it is possible to locally correlate changes in temperature gradient with the presence of massive anhydrite in the cutting samples, this simplification will not affect the estimates of thermal cap thickness. (2) The thermal conductivity in either rock type is independent of temperature and pressure. (3) The conductive heat flow is constant between depths where temperature is measured.

If a well interval of length ΔZ consists of n layers with thermal conductivity κ_i, and thickness h_i, i = 1, n, and the temperature difference over that interval is ΔT, then the conductive heat flow, Q, is given by:

$$Q_{cond} = \frac{\Delta T}{\Delta Z} \left(\frac{1}{\Delta Z} \cdot \sum_{i=1}^{n} \frac{h_i}{\kappa_i} \right)^{-1} . \qquad (2)$$

If each layer is either sand or shale, with conductivity κ_s or κ_{sh} respectively, and ΔZ_s is the sum of the thicknesses of the sand layers, then

$$Q_{cond} = \frac{\Delta T}{\Delta Z}\left[\frac{1}{\Delta Z}\cdot\left(\sum_{sand}\frac{h_i}{\kappa_s}+\sum_{shale}\frac{h_i}{\kappa_{sh}}\right)\right]^{-1}, \tag{3}$$

and

$$Q_{cond} = \frac{\Delta T}{\Delta Z}\left[\frac{\Delta Z_s}{\Delta Z\kappa_s}+\left(1-\frac{\Delta Z_s}{\Delta Z}\right)\cdot\frac{1}{\kappa_{sh}}\right]^{-1}. \tag{4}$$

$$\frac{Q_{cond}}{\kappa_{sh}} = \frac{\Delta T}{\Delta Z}\cdot\frac{1}{1+(\alpha-1)R} = \text{relative conductive heat flow}, \tag{5}$$

where $\alpha = \frac{\kappa_{sh}}{\kappa_s}$ and R = sand percentage.

The relative conductive heat flow for 12 wells changes as a function of depth (Fig. 15). The conductive heat flow is nearly constant in the upper section of most wells and then decreases rapidly with increasing depth.

Convection is inferred to be the important mechanism of heat flow below the level where the conductive heat flow decreases. An estimate of the thickness of the thermal cap is provided in Fig. 15. The depth differs considerably at adjacent wells but becomes increasingly shallow away from the Salton Sea, consistent with the westward dip of the reservoir strata. The Sinclair, Magmamax 3, and River Ranch wells appear to be anomalous. If we

compare the depths shown in Fig. 15 with previous lithologic observations, we see that the thermal cap is, in general, somewhat thicker than the lithologic cap, and the the upper portion of the clastic sediments appears to transfer heat largely through conduction, despite the inferred high porosity and permeability of the sediments.

A comparison of well logs and temperature gradients for Elmore No. 1 (Fig. 16) suggests that convection is lithology controlled. Modest gradients are shown at depths from 500 to 1000 m in the zone of thin sand beds, but near zero gradients exist below 1400 m where sand beds are thick.

We plotted a north-south cross section and compared the reservoir character with the thickness of the thermal cap (Fig. 17). Towse and Palmer (1976) provided the estimate of reservoir quality based on an interpretation of inferred permeability and continuity of rock units. Two observations are important. First, in all the wells the base of the thermal cap is within the zone where the percentage of sand is high (> 20%). Second, in several wells (Magmamax No. 3, Elmore No. 1, IID No. 2, and Sportsman No. 1) the base of the thermal cap coincides with the first appearance of high reservoir quality ($\geq$ 4). These observations support the idea of lithologic control of heat transport mechanisms within the reservoir. The dominant controls are probably sand bed thickness and lateral continuity of intervening shale beds, although the fracture permeability of shales may be locally significant.

Vertical convection does not occur in some permeable sand zones indicating that vertical permeability is small in the upper part of the section. Several lines of evidence also suggest that individual shale beds can effectively reduce the vertical permeability and thereby prevent large-scale convection

cells within the zone of convective flow. Towse and Palmer (1976) and Tewhey (1977) identified several major shale beds over 14 m thick in the reservoir sands which would surely provide impermeable barriers to convective flow if they are not extensively fractured.

Kendall (1976) provides support for the concept of a reservoir split into several hydrologic systems. She found that extensive oxygen and carbon isotope exchange occurred between geothermal brines and reservoir rock and that several isotope inversions can be correlated with stratigraphic horizons. This correlation suggests that water transport in the interval between 300 and 900 m is largely lateral and stratigraphically controlled. Consistent composition below 900 m indicates that the water there is more thoroughly mixed, perhaps as a result of the extensive fractures. In addition, minerals in the larger fractures have approximately the same chemical and isotopic compositions as minerals in the wall rocks, indicating that the large fractures were not major avenues of water transport.

More evidence for a lack of large-scale vertical transport of fluids and, therefore, no large-scale convection cells comes from pressure measurements within the wells, and well interference tests. The hydrostatic pressure-versus-depth profile in the field is consistent with a constant fluid density of 1 g/cm^3. This observation precludes large convective movements, but, as was pointed out by Helgeson (1968), smaller convection geometries cannot be tested because of the uncertainty in the pressure measurements. Morse and Thorsen (1978) analyzed well interference data and noted that wells 7 m apart did not communicate across a major shale break. They concluded that the vertical permeability in the region is very low.

An analysis of the conditions required for convection in a porous medium

supports the hypothesis that the vertical heat transport could result from convection in individual sand layers (at least in the upper reservoir). Elder (1967) did numerical and experimental studies of convection in a porous medium. He found that the heat transport within a single layer is controlled by a modified Rayleigh number, η, and convection only occurs if η is greater than 40.

$$\eta = \frac{\kappa \alpha \ \Delta T \ gH}{\kappa_m \nu} \quad , \tag{6}$$

where κ = Permeability of the layer

α = Coefficient of volume expansion of the fluid

g = Absolute value of acceleration due to gravity

κ_m = Thermal diffusivity of the saturated medium

ν = Kinematic viscosity of the convecting fluid

H = Thickness of the layer

ΔT = Temperature contrast across the layer

To determine accurately whether convection will develop in a sand of a given thickness, permeability, and depth, the variation of physical properties of the convecting fluid as a function of temperature and pressure must be investigated. Convection depends strongly on the coefficient of expansion, kinematic viscosity, and the thermal diffusivity of the saturated medium, each highly dependent on temperature. The (conjugate) variation of these three parameters changes η and makes convection much stronger when the temperature increases. By considering this variation, we can show that sand units of a given thickness and permeability are more likely to support convection if

buried to a depth where the temperature was high.

For this report, we assumed the convecting fluid is pure water and the reservoir sands are quartzitic sandstones. The permeability in upper reservoir rocks was estimated to be 500 md, and permeability in lower reservoir rocks was estimated to be 180 md (Morse and Thorsen, 1978).

Using Elder's criterion for η, we prepared tables in which the thickness of sand necessary for convection is given as a function of permeability, temperature, and geothermal gradient. In Table 2 is the required thickness as a function of temperature for two geothermal gradients and permeabilities of 180 md, representative of the lower reservoir, and 500 md, representative of the upper reservoir. We chose the geothermal gradients to represent the range of possible gradients before convection starts.

Three major points emerge from the analysis. First, temperature is a very important parameter. Given a permeability of 500 md and a gradient of 0.33°C/m, it would require a bed 284 m thick to convect at 50°C, but at 300°C, a bed 31 m thick would support convection. Even under a high temperature gradient and high permeability, a sand unit would have to be thicker than 60 m to support convection at temperatures less than 200°C. Second, in the upper reservoir, convection probably occurs in individual sand units. Temperatures greater than 200°C will produce convection in sand units varying in thickness from 30 to 100 m, depending on the geothermal gradient. Finally in the lower reservoir, convection is unlikely in individual sand units because of their lower permeability. Under high geothermal gradients and at 200°C, a sand unit must be 107 m thick for convection to occur. This approaches the upper limit of thickness for a sand bed in the Salton Sea Geothermal Field. Therefore, we would expect fracture

permeability to be the dominant factor facilitating convection in deep reservoir rocks.

Horizontal heat transport within the reservoir

It is possible that a much larger scale of horizonal convection is superimposed on the small-scale convection, which controls the vertical heat transport in the reservoir. High lateral permeability occurs even where the reservoir is segmented vertically by shale beds. SP logs of 350-ft (100-m) intervals from nine geothermal wells placed in juxtaposition to emphasize similiarities (Fig. 18) support the idea of widespread continuity of individual sand beds throughout the area. Thus, the lateral permeability within the reservoir is much greater than the vertical, and the possibility of large-scale lateral flow exists.

If the temperature at the base of the thermal cap in several wells is plotted as a function of the value of the magnetic anomaly at each well head, the result is a nearly straight line (Fig. 19). This unlikely correlation lends further support to a horizontal flow model. The magnetic anomaly at the Salton Sea Geothermal Field is caused by intrusions, which are probably the source of heat for the field. Therefore, the value of the magnetic anomaly can be used as a rough index of the distance from the source of heat. The temperature at the base of the cap apparently decreases monotonically with distance from the source of the heat (Fig. 19), and this is surprising if we consider tnat the depth to the base of the cap is quite irregular. However, it is consistent with a model of large-scale horizontal flow beneath the lithologic cap. Fluid rises above a localized heat source and spreads

laterally away from the source losing heat to the impermeable cap rock. If this model of predominantly horizontal flow is correct, then the high salinity brine inferred from the resistivity data could be the total mass of water that has flowed through the system. In our next paper we will model the heat transport associated with this lateral flow, and compare it with more detailed observations on the temperature distribution within the field.

SUMMARY OF CHARACTERISTICS

Geology

1. Sediments within the field can be characterized as a three layer sequence of cap rock, slightly altered reservoir rock and more extensively altered reservoir rock. The sharp transition between the cap rock and the underlying reservoir rock is interpreted to represent the boundary between lacustrine sediments deposited in the isolated Salton Trough, and earlier marine sediments deposited in the Gulf of California.
2. The cap rock is a variably thick, low permeability rock overlying the reservoir rock. In the upper 200 m, it consists of unconsolidated clay, silt, sand, and gravel. Below 200 m, it consists primarily of anhydrite-rich evaporite layers.
3. The slightly altered reservoir rocks were subject to silicification and clay mineral reactions; however, these alterations did not change the petrophysical properties.
4. Epidote and silica are the principal pore filling minerals produced during high temperature alteration. They replace calcite and anhydrite and a

reduction of porosity and permeability within the altered reservoir zone results.

5. Anhydrite veins reveal two or more episodes of fracturing and deposition indicating that the loss of permeability resulting from hydrothermal alteration is countered by the continuous development of new fractures.
6. Correlations of data from well logs indicate that the sediments form a broad syncline with an east-west axis approximately perpendicular to the axis of the Salton Trough.
7. Igneous activity is evidenced by five rhyolite buttes within the Salton Sea Geothermal Field. Basaltic and silicic dikes and sills are observed at depths of 1 to 2 km within the field (Robinson et al., 1976).

Geophysics

1. The field is associated with a local gravity high, probably resulting from intrusion of dike material, or of hydrothermal alteration of the sediment, or of both (Biehler et al., 1964).
2. The field is associated with a magnetic anomaly that probably reflects the presence of igneous material near the surface (Griscom and Muffler, 1971; Kelley and Soske, 1936).
3. The resistivity anomaly probably reflects the boundary of the saline brine. The conductance of the sedimentary sequence is greatest in the area of the drilled field, but a broad area of high conductance extends along the axis of the valley (Meidav et al., 1976; Kasameyer, 1976).
4. Seismic refraction data reveal the presence of high velocity material within 1 km of the surface (Frith, 1978).

5. Numerous earthquakes indicate that the area is tectonically active (Schnapp and Fuis, 1977).
6. Interpretations of resistivity surveys, seismic refraction data, earthquake locations, and ground magnetic surveys are suggestive of the existence of several steeply dipping faults within the field (Muffler and White, 1968; Babcock, 1971; Meidav and Furgerson, 1972; Towse, 1975; Gilpin and Lee, 1978; Frith, 1978).

Geothermal

1. Equilibrium temperature analysis indicates that the field is characterized by extremely high temperatures at depth. Temperatures at a depth of 2 km are 200°C higher than temperatures at similar depths in nongeothermal areas within the valley.
2. Within the field, temperature profiles are characterized by high temperature gradients near the surface. There is a dramatic reduction in gradient at a depth of approximately 700 m.
3. At the margin of the field, temperature profiles are characterized by low gradients at the surface and an increase in temperature gradient with depth.
4. Surface gradients within the field are fairly constant, averaging 0.36°C/m. Surface gradients drop off rapidly to the regional value as the margin of the field is approached.
5. The thermal cap does not necessarily conform in thickness to the lithologic cap; it varies irregularly. However, the temperature at the base of the cap varies smoothly with distance from the volcanic buttes.

6. Heat transfer mechanisms can be modeled as a three layer system. Layer one, the upper thermal cap, is impermeable to fluid flow and has a high temperature gradient consistent with conduction. Layer two, still within the thermal cap but below the lithologic cap rock, has an increase in high-conductivity sand units that produce a lower temperature gradient. Layer three, below the thermal cap, is characterized by low thermal gradients consistent with convective flow of pore fluid.
7. A variety of evidence suggests that vertical convective motion within the reservoir is confined to small units. Vertical permeability is too low to allow for large-scale convection cells. Convection in the upper part of the reservoir is limited to individual sand bodies. Minor fractures in the lower reservoir allow for more extensive convective patterns. Major faults have not served as avenues of fluid and heat transport (Kendall, 1976).
8. Superimposed on the small-scale convection could be a large-scale horizontal flow that transfers heat from the area of the buttes to the margins of the field.

A schematic section of the field, which relates the geological characteristics and the heat transfer characteristics, is seen in Fig. 20. Geologically, the section can be broken down into four layers (cap rock, slightly altered reservoir rock, highly altered reservoir rock, and zone of intrusion). The impermeable cap rock is underlain by the dominantly sand reservoir. The lower portion of the reservoir has undergone hydrothermal alteration, which changed the petrophysical properties. Basaltic and silicic dikes penetrate to within 1 km of the surface. On the basis of thermal properties, the field can be broken down into three layers. The thermal cap

is characterized by conductive heat transfer and includes the cap rock and an upper portion of the sand reservoir where the sand beds are thin. The convective zone includes the major portion of the sand reservoir. Small-scale cellular convection is superimposed upon a large-scale lateral flow of pore fluid. The heat source region corresponds to the zone of intrusion. The rate of heat release in this region is a function of the rate of intrusion. In a future paper we will use these observations as a basis for establishing and evaluating a system model.

ACKNOWLEDGMENTS

We benefited from discussions with numerous colleagues, most notably Larry Owen, Jack Howard, Jon Hanson, and Don Towse. The assistance of Lila Abrahamson, of the Technical Information Department at LLNL, in getting the manuscript into final form is appreciated. We acknowledge support of the Office of Basic Energy Sciences and the Division of Geothermal Energy of the Department of Energy.

This work was performed under the auspices of the U.S. Department of Energy by Lawrence Livermore National Laboratory under contract No. W-7405-Eng-48.

REFERENCES

Babcock, E. A., 1971. Detection of active faulting using oblique infrared aerial photography in the Imperial Valley of California, Geol. Soc. Am. Bull., 82: 3189-3196.

Batzle, M. L. and Simmons, G, 1976. Microfractures in rocks from two geothermal areas, Earth Plant. Sci. Lett., 30: 71-93.

Berner, R. A., 1971. Principles of Chemical Sedimentology. McGraw-Hill, New York, N.Y.

Biehler, S., 1971. Gravity studies in the Imperial Valley. In: Cooperative Geological-Geophysical Investigations of Geothermal Resources in the Imperial Valley Area of California. University of California, Riverside, Calif.

Biehler, S., Kovach, R. L. and Allen, C. R., 1964. Geophysical framework of northern end of Gulf of California Structural Province, Am. Assoc. Petrol. Geol., Memo No. 3: 126-143.

Biehler, S. and Lee, T., 1977. Final report on a resource assessment of the Imperial Valley, DLRI Report No. 10. University of California, Riverside, Calif.

Chan, M. A. and Tewhey, J. D., 1977. Subsurface structure of the southern portion of the Salton Sea Geothermal Field, UCRL-523554. Lawrence Livermore National National Laboratory, Livermore, Calif.

Combs, J. and Hadley, D., 1977. Microearthquake investigation of the Mesa Geothermal Anomaly, Imperial Valley, California, Geophysics, 42: 17-33.

Dibblee, T. W., Jr., 1954. Geology of the Imperial Valley Region, California, Pt. 2. In: R. H. Jahns (Editor), Geology of Southern California, Calif. Div. Mines Bull. No. 170, pp. 21-28.

Downs, T. and Woodward G. D., 1961. Middle Pleistocene extension of the Gulf of California into the Imperial Valley, Geol. Soc. Am. Abst. Spec. Paper No. 68, p. 21.

Dutcher, L. C., Hardt, W. F. and Moyle, W. R., Jr., 1972. Preliminary appraisal of ground water in storage with reference to geothermal resources in the Imperial Valley Area, California, U.S. Geolog. Surv. Circ. 649.

Elder, J. W., 1967. Steady free convection in a porous medium heated from below, J. Fluid Mech., 27: 29.

Elders, W. A., Rex, R. W., Meidav, T., Robinson, P. T. and Biehler, S., 1972. Crustal spreading in Southern California, Science, 178: 15-24.

Elders, W. A. and Biehler, S., 1975. Gulf of California rift system and its implication for the tectonics of Western North America, Geology, 3(2): 85.

Facca, G., 1973. The structure and behavior of geothermal fields. In: H. C. H. Armstead (Editor), Geothermal Energy, Review of Research and Development. United Nations Educational, Scientific and Cultural Organization, Paris, pp. 61-69.

Facca, G. and Tonani, F., 1967. The self-sealing geothermal field, Bull. Volcanol., 30: 271-273.

Frith, R. B., 1978. A seismic refraction investigation of the Salton Sea Geothermal area, Imperial Valley California. M.S. Thesis, University of California, Riverside, Calif., 94 pp. (unpublished).

Gilpin, B. and Lee, Tien-Chang, 1978. A microearthquake study in the Salton Sea Geothermal area, California, Bull. Seism. Soc. Am., 68: 441-450.

Grindley, G. W. and Browne, P. R. L., 1976. Structural and hydrological factors controlling the permeabilities of some hot-water geothermal wells. In: Proc. Second United Nations Symp. on Development and Use of Geothermal Resources, vol. 1. Lawrence Berkeley Laboratory, Berkeley, Calif., pp. 379-386.

Griscom, A. and Muffler, L. J. P., 1971. Aeromagnetic map and interpretation of the Salton Sea geothermal area, California, U.S. Geol. Survey, Geophys. Invest. Map GP 754.

Hamilton, W., 1961. Origin of the Gulf of California, Geol. Soc. Am. Bull., 72: 1307-1318.

Helgeson, H. C., 1968. Geologic and thermodynamic characteristics of the Salton Sea geothermal system, Am. J. Sci., 266(3): 129-166.

Hill, D. P., 1977. A model for earthquake swarms, J. Geophys. Res., 82: 1347-1352.

Hill, D. P., Mowinckel, P. and Peake, L. G., 1975. Earthquake active faults and geothermal areas in the Imperial Valley, California, Science 188: 1306-1308.

Johnson, C. E., 1979. I. CEDAR--An approach to the computer automation of short-period local seismic networks; II. Seismotectonics of the Imperial Valley of Southern California, Ph.D. dissertation, California Institute of Technology, Pasadena, Calif.

Kasameyer, P. W., 1976. Preliminary interpretation of resistivity and seismic refraction data from the Salton Sea Geothermal Field, UCRL-52115. Lawrence Livermore National Laboratory, Livermore, Calif.

Keller, G. V. and Frischknecht, F. C., 1966. Electrical Methods in Geophysical Prospecting. Pergamon Press, New York, N.Y.

Kelley, V. C. and Soske, J. L., 1936. Origin of the Salton volcanic domes, Salton Sea, California, J. Geol., 44: 496-509.

Kendell, C., 1976. Petrology and stable isotope geochemistry of three wells in the Buttes area of the Salton Sea Geothermal Field, Imperial Valley California, U.S.A. M.S. Thesis, University of California, Riverside, Calif. (unpublished).

Lee, T. and Cohen, L., 1977. Onshore and offshore measurements of temperature gradients in the Salton Sea geothermal area California, UCR/I6PP-77/22. University of California, Riverside, Calif.

Lofgren, B. E., 1978. Salton Trough continues to deepen in Imperial Valley, California, Trans. Am. Geophys. Union, 59: 1051.

Lomnitz, C., Mooser, F., Allen, C., Brune, J. N. and Thatcher, W., 1970. Seismicity of the Gulf of California region, Mexico--preliminary results, Geofis. Int. 10: 37.

Magma Power Company, 1979. Personal communication.

McDowell, S. D. and McCurry, M., 1977. Active metamorphism in the Salton Sea Geothermal Field, California: mineralogical and mineral chemistry changes with depth and temperature in sandstone, Geol. Soc. Am. Abstr. Prog., 9(7): 1088.

McDowell, S. D. and Elders, W. A., 1979. Geothermal metamorphism of sandstone in the Salton Sea Geothermal System, UCR/I6PP-79-25. Inst. Geophys. Planet. Phys., University of California, Riverside, Calif.

Meidav, T. and Fergerson, R., 1972. Resistivity studies of the Imperial Valley geothermal area, California, Geothermics, 1: 47-62.

Meidav, T., West, R., Katzenstein, A. and Rostein, Y., 1976. An electrical resistivity survey of the Salton Sea Geothermal Field, Imperial Valley California, UCRL-13690. Lawrence Livermore National Laboratory, Livermore, Calif.

Morse, J. G. and Thorson, L. D., 1978. Reservoir engineering study of a portion of the Salton Sea Geothermal Field, Geotherm. Resources Council Trans., 2: 471-474.

Muffler, L. J. P. and White, D. E., 1968. Origin of CO_2 in the Salton Sea geothermal system, Southeastern California, U.S.A.. In: Proc. 23rd Int. Geol. Cong., Prague, 97(Symp. 2): 185-194.

Muffler, L. J. P. and White, D. E., 1969. Active metamorphism of upper Cenozoic sediments in the Salton Sea Geothermal Field and the Salton Trough, Southeastern California, Geol. Soc. Am. Bull., 80: 157-182.

Nathenson, M. and Muffler, L. J. P., 1975. Geothermal Resources in Hydrothermal convection systems and conduction dominated areas. In: Assessment of Geothermal Resources of the United States, U.S. Geological Survey, Washington D.C., Circ. 726.

Palmer, T. D, 1975. Characteristics of geothermal wells located in the Salton Sea Geothermal Field, Imperial County, California, UCRL-51976. Lawrence Livermore National Laboratory, Livermore, Calif.

Randall, W., 1974. An analysis of the subsurface structure and stratigraphy of the Salton Sea geothermal anomaly, Imperial Valley, California. Ph.D. Thesis, University of California, Riverside, Calif. (unpublished).

Renner, J. L., White, D. E. and Williams, D. L., 1975. Hydrothermal convection systems. In: Assessment of Geothermal Resources of the United States, U.S. Geological Survey, Washington D.C., Circ. 726.

Robinson, P. T., Elders, W. A. and Muffler, L. J. P., 1976. Quaternary Volcanism in the Salton Sea Geothermal Field, Imperial Valley California, Geol. Soc. Am. Bull., 87: 347-360.

Schnapp, M and Fuis, G., 1977. Preliminary catalog of earthquakes in the Northern Imperial Valley, October 1, 1976 to December 31, 1976. U.S. Geol. Surv. Seism. Lab., Pasadena, Calif.

Skinner, B. J., White, D. E., Rose, H. J. and Mays, R. E., 1967. Sulfides associated with the Salton Sea Geothermal brine, Econ. Geol., 62(3): 316-330.

Storre, B. and Nitsch, K. H., 1972. Die reaktion 2 zoisite + 1 CO_2 ⇌ 3 anorthite + 1 calcite + 1 H_2O, Contr. Mineral. Petrol., 35: 1-10.

Sylvester, A. G., 1979. Earthquake damage in Imperial Valley, California May 18, 1940, as reported by T. A. Clark, Bull. Am. Seis. Soc., 69: 547-568.

Tewhey, J. D., 1977. Geologic characteristics of a portion of the Salton Sea Geothermal Field, UCRL-52267. Lawrence Livermore National Laboratory, Livermore, Calif.

Towse, D., 1975. An estimate of the geothermal energy resource in the Salton Trough California, UCRL-51851. Lawrence Livermore National Laboratory, Livermore, Calif.

Towse, D. F. and Palmer, T. D., 1975. Summary of geology at the ERDA-Magma-SDG&E geothermal test site, UCID-17008. Lawrence Livermore National Laboratory, Livermore, Calif.

Van de Kamp, P. C., 1973. Holocene continental sedimentation in the Salton Basin, California: a reconnaissance, Geol. Soc. Am. Bull., 84: 827-848.

Weaver, C. S. and Hill, D. P., 1978. Earthquake swarms and local crustal spreading along major strike-slip faults in California, Pure Appl. Geophys., 177: 51-64.

White, D. E., 1968. Environments of generation of some base metal ore deposits, Econ. Geol., 63(4): 301-335.

Younker, L. and Kasameyer, P. W., 1978. A revised estimate of recoverable thermal energy in the Salton Sea Geothermal resource area, UCRL-52450. Lawrence Livermore National Laboratory, Livermore, Calif.

TABLE 1

Near-surface temperature gradient associated with geothermal wells in the Salton Sea Geothermal Field, and the maximum depth to which the gradient is valid.

Well	Gradient (°C/m)	Maximum depth, D, of valid gradient (m)	Comments
River Ranch No. 1	≤ 0.4	$D < 300$	May be 1.6°C/m
IID No. 1	0.316 ± 0.007[a]	$700 < D < 850$	
IID No. 2	0.39 ± 0.02	$D < 300$	Based on two points
IID No. 3	0.366 ± 0.006[a]	$460 < D$	
State No. 1[b]	0.40 ± 0.05[a]	$300 < D < 600$	
Elmore No. 1	0.391 ± 0.008[a]	$600 < D < 650$	
Magmamax No. 1	0.457 ± 0.009[a]	$460 < D < 525$	Three data sets, 1972
Magmamax No. 2	0.368 ± 0.008[a]	$570 < D < 650$	Three data sets, 1974-76
Magmamax No. 3[c]			
Magmamax No. 4[d]	0.350 ± 0.04[a]	$120 < D < 180$	Six data sets, 1973 to 1976
Woolsey No. 1	0.463 ± 0.010[a]	$400 < D < 430$	Three data sets, 1974 to 1976
Sinclair No. 3	0.11 ± 0.007	$D \curvearrowright 690$	
Sinclair No. 4	≤ 0.11	$D < 650$	Based on two points
Sportsman	0.337 ± 0.007[a]	$600 < D < 750$	

[a]Gradient estimated from statistical analysis.

[b]State No. 1. Data variability greatly exceeds uncertainty of $\pm$ 5°C/m in shallow zones. Best fit and standard deviation were determined subjectively.

[c]The data set representing equilibrium temperatures cannot be determined. The gradient from Magmamax No. 4 was used.

[d]The gradient increases to 0.58°C/m and is constant for depth ranging from 150 to 350 m. The average gradient from 0 to 350 m is 0.49 °C/m.

TABLE 2

Thickness necessary to support convection.

	Necessary thickness at assumed gradients			
	Permeability of 180 md		Permeability of 500 md	
Assumed temperature (°C)	0.33°C/m (m)	0.16°C/m (m)	0.33°C/m (m)	0.16°C/m (m)
0	1385	1992	832	1195
50	474	681	284	408
100	247	355	148	213
150	157	225	94	135
200	107	154	64	92
250	78	112	47	67
300	52	75	31	45

Figure Captions

Fig. 1. Location of the Salton Sea Geothermal Field and nearby faults in the Imperial Valley (after Elders et al., 1972). Basement rocks are indicated by stippling. The inset shows locations of wells in the field.

Fig. 2. East-west cross section through the Magmamax and Woolsey wells in the Salton Sea Geothermal Field. The three rock types, i.e., cap rock, slightly altered reservoir rock, and hydrothermally altered rock, are classifications based on petrographic analysis. Boundaries between rock types are those determined in this report. The orientation of strata in the reservoir rock is shown by dashed lines.

Fig. 3a. Temperature versus CO_2 content plotted at P_{fluid} = 2kb for the CaO-Al_2O_3-SiO_2-CO_2-H_2O system modified from Storre and Nitsch (1972). The shaded arrow represents a possible reaction path, with depth, for the Salton Sea Geothermal Field that is consistent with petrologic observations. The calcite-anorthite-quartz (CAQ) triangle is used to depict phase relations. 3b. Detail of CAQ triangle.

Fig. 4. Measured porosity versus depth for cores from five geothermal wells in the Salton Sea Geothermal Field.

Fig. 5. Calcite and epidote veins in shale from > 900-m depths in the Salton Sea Geothermal Field. Ion microprobe-traverses were made across zoned anhydrite grains to determine the geochemical basis for differences in luminescent intensity. The position of data points in the graph are seen on the ion microprobe-transverse. Positive concentration-anomalies of Y, Ce, and La correspond to zones of yellow luminescence.

Fig. 6. Spontaneous potential (SP) log correlations of five wells extending north to south from Elmore No. 1 to Sinclair No. 3 in the Salton Sea Geothermal Field.

Fig. 7. Bouguer gravity anomaly map of the area near the Salton Sea Geothermal Field (after Biehler, 1971). Heavy solid line shows the position of a seismic refraction profile (refer to Fig. 10). The contour intervals is 2.5 milligals.

Fig. 8. Aeromagnetic map of the area near the Salton Sea Geothermal Field (after Griscom and Muffler, 1971). The contour interval is 25 gammas.

Fig. 9. Conductance map for area near the Salton Sea Geothermal Field (after Kasameyer, 1976). Open circles indicate the location of the soundings. Conductance is in siemens.

Fig. 10. Seismic refraction profile running from Obsidian Butte on the east to the Alamo River on the west (after Frith, 1978). The position of the profile is indicated on the gravity anomaly map (Fig. 7). Velocities are in km/s.

Fig. 11. Location of earthquake epicenters in the Imperial Valley for the period October 1, 1976 through December 31, 1976 (after Schnapp and Fuis, 1977). The solid triangles are seismograph stations in the Imperial Valley network installed in 1973. Solid circles are the seismograph stations installed in November 1976. Open circles and dots are the observed epicenters. Tentative fault locations are shown in broken lines.

Fig. 12. Equilibrium temperature profiles for 13 wells in the Salton Sea Geothermal Field. a. and b. Wells from the northern part of the field. c. and d. Wells from the southern part of the field. The data for these profiles are from Helgeson, 1968; Randall, 1974; Palmer, 1975; and Magma Power Company, 1979.

Fig. 13. A map of the spatial character of the geothermal anomaly. Each measurement point is represented by three symbols: a dot showing the location, a number indicating the near surface gradient, and a letter representing the character of the temperature versus depth curve. Upper case letters indicate deep wells. Wells marked A have a moderately high uniform heat flow in the upper few hundred metres, and a nearly isothermal zone at depth. Wells marked B have a nearly constant low heat flow throughout their depth. Wells marked C have low heat flow near the surface, but their gradient increases with depth. Lower case letters represent shallow hole data (Lee and Cohen, 1977) with corresponding characteristics. Holes marked a or b have high or low gradients, respectively. The shallow wells are not deep enough to distinguish between B and C behavior. The solid lines represent the approximate boundaries of regions with similar characteristics, indicated by A, B, or C.

Fig. 14. Surface gradient versus temperature at a depth of 1000 m for 9 wells in the Salton Sea Geothermal Field. The line represents the temperature that would be at 1000 m if the gradient were constant.

Fig. 15. Thermal gradients versus depth for 12 wells in the Salton Sea Geothermal Field. The interval gradient is indicated by a dashed line. The gradient corrected for the sand conductivity is indicated by a solid line. The depths at which the conductive heat flow has decreased by 30 to 40% are indicated by arrows. Convection is interpreted as a mechanism for significant heat transfer below these points. If the decrease in conductive heat flow occurs between widely-spaced temperature measurements, the arrow is placed at a change of lithology between the observation depths. The depth uncertainty is greater than 30 m in all cases. The data for State of California No. 1 are (left) from the State of California Division of Oil and Gas and (right) from Helgeson (1968).

Fig. 16. The percentage of sand and the interval gradients for the Elmore No. 1 well in the Salton Sea Geothermal Field.

Fig 17. A north-south section across the Salton Sea Geothermal Field showing that the thermal cap does not coincide with the lithologic cap. Sandstone percentage, a subjective measure of reservoir quality (Towse, 1976), and the thickness of the base of the thermal cap are shown for six wells. From south to north, the wells are Sinclair No. 4, Woolsey No. 1, Magmamax No. 3, Elmore No. 1, IID No. 2, and Sportsman No. 1.

Fig. 18. Data from SP logs of nine geothermal wells with markers set at 100-m intervals (after Chan and Tewhey, 1977). The marker bed occurs at a different depth in each well, and the logs were displaced vertically so that similarities among wells can be seen.

Fig. 19. A cross plot of temperature at the base of the thermal cap versus amplitude of the magnetic anomaly at the surface for 13 wells. The systematic variation suggests that there is a physical relationship between the source of the magnetic anomaly and the source of the heat.

Fig. 20. The relationship between the lithology and the heat transfer characteristics at different zones from cap rock down to intrusion.

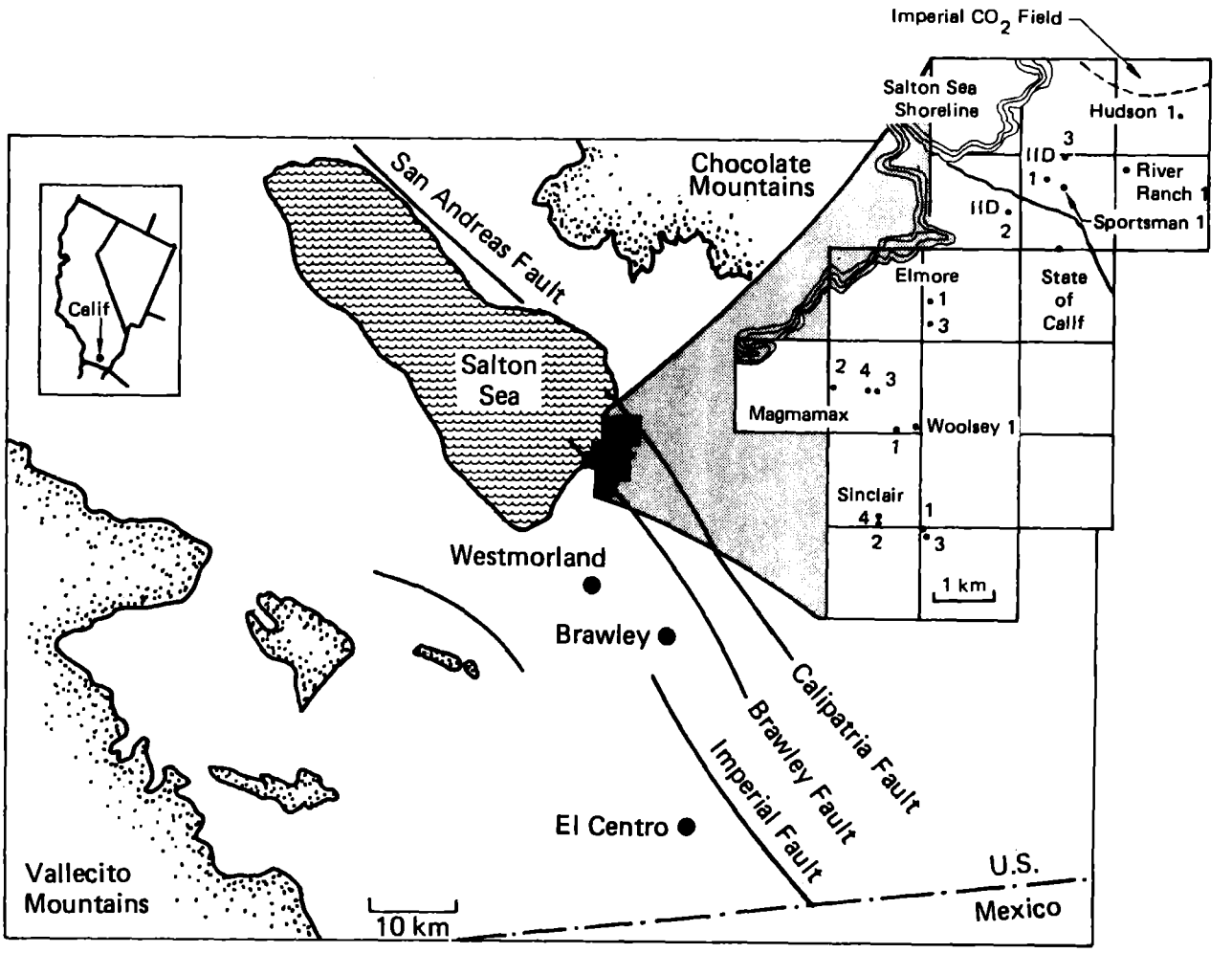

Younker--Fig. 1

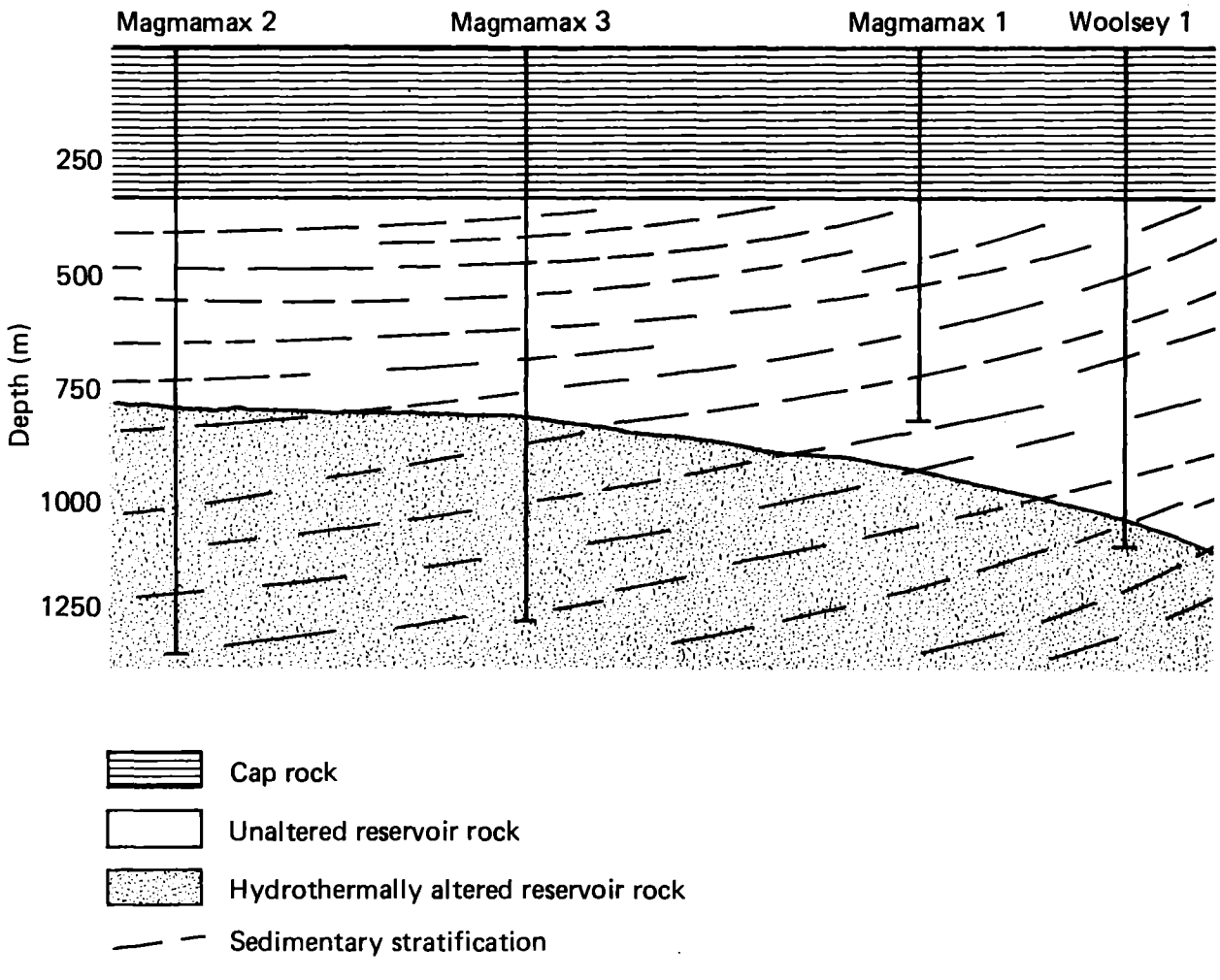

Younker--Fig. 2

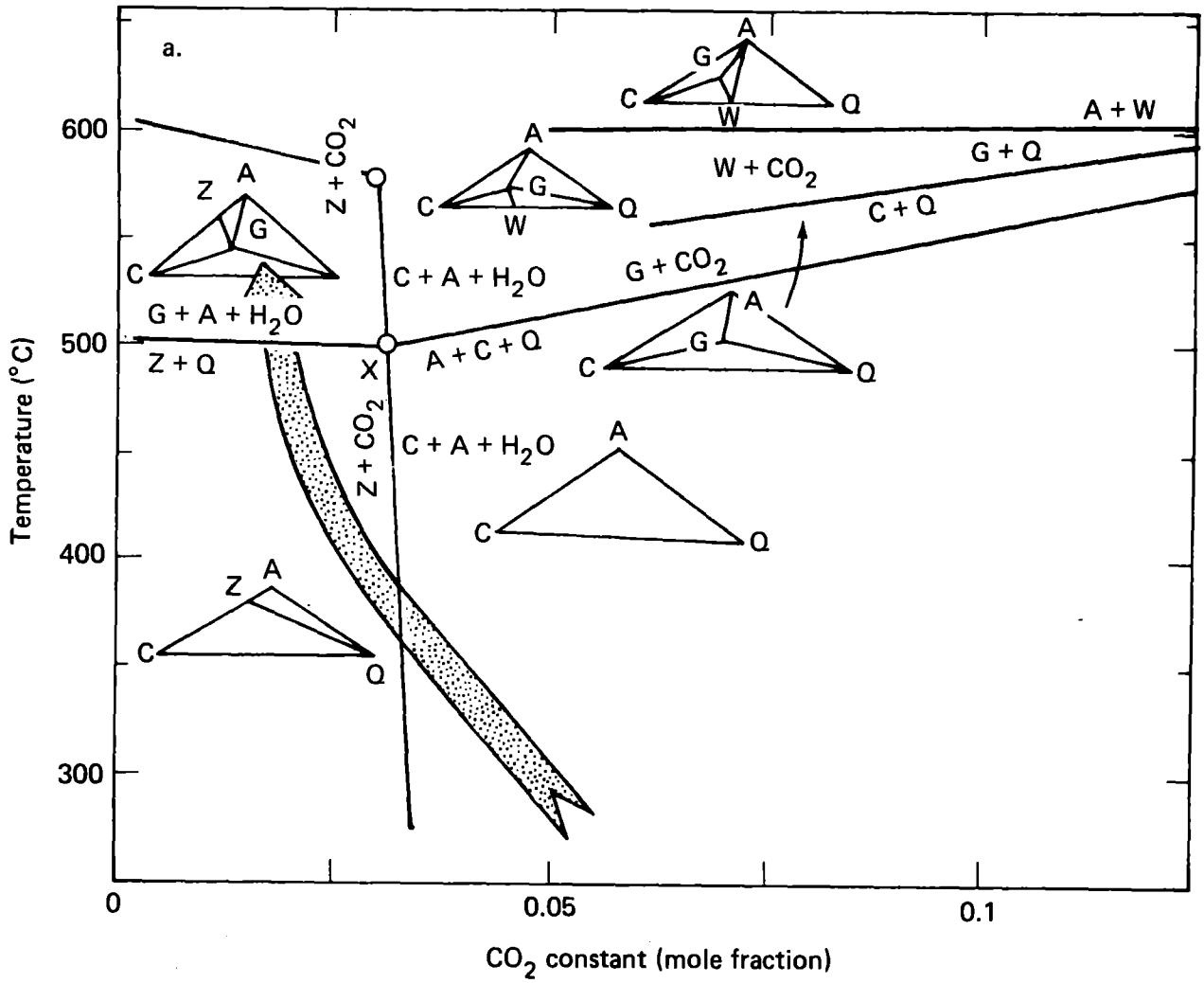
a.
600
500
400
300
Temperature (°C)
0
0.05
0.1
CO_2 constant (mole fraction)
A
G
C
W
Q
A + W
W + CO_2
G + Q
C + Q
Z + CO_2
Z
C + A + H_2O
G + A + H_2O
G + CO_2
Z + Q
X
A + C + Q
C + A + H_2O
Z + CO_2

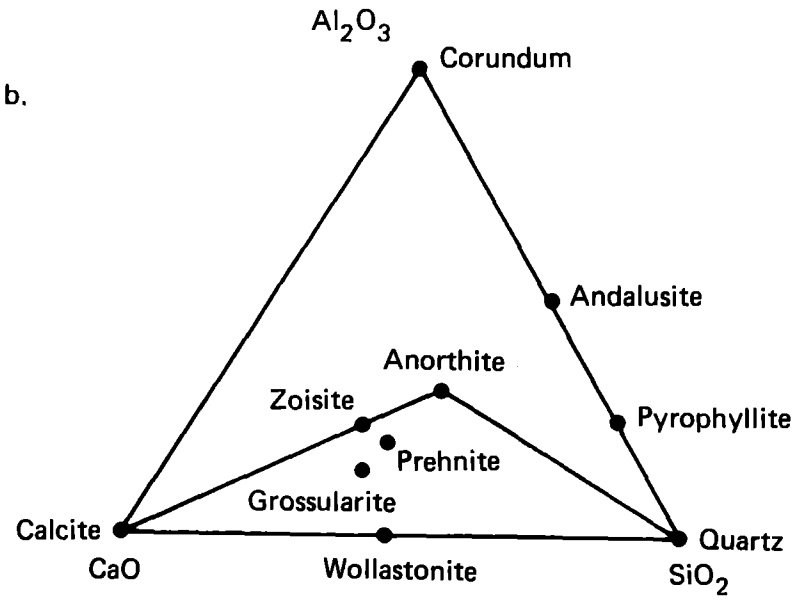
b.
Al_2O_3
Corundum
Andalusite
Anorthite
Zoisite
Pyrophyllite
Prehnite
Grossularite
Calcite
CaO
Wollastonite
Quartz
SiO_2

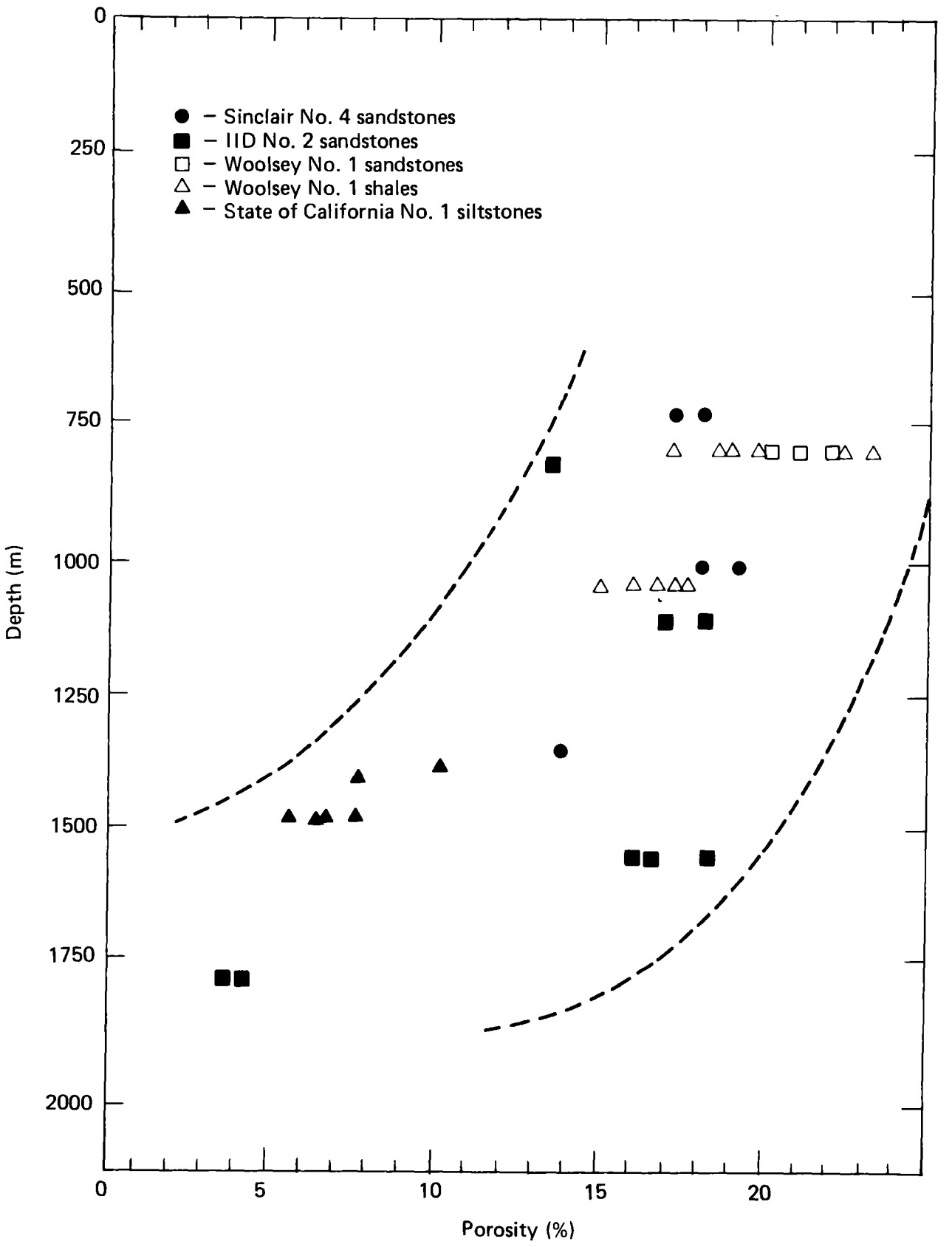

Younker--Fig. 4

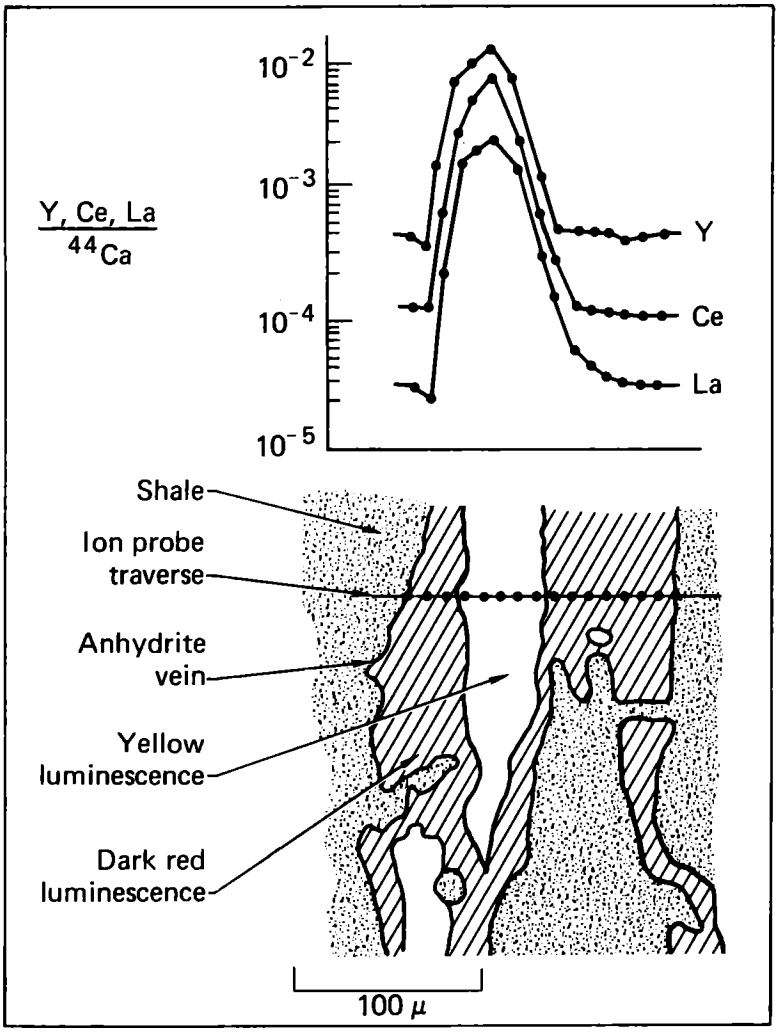

Younker--Fig. 5

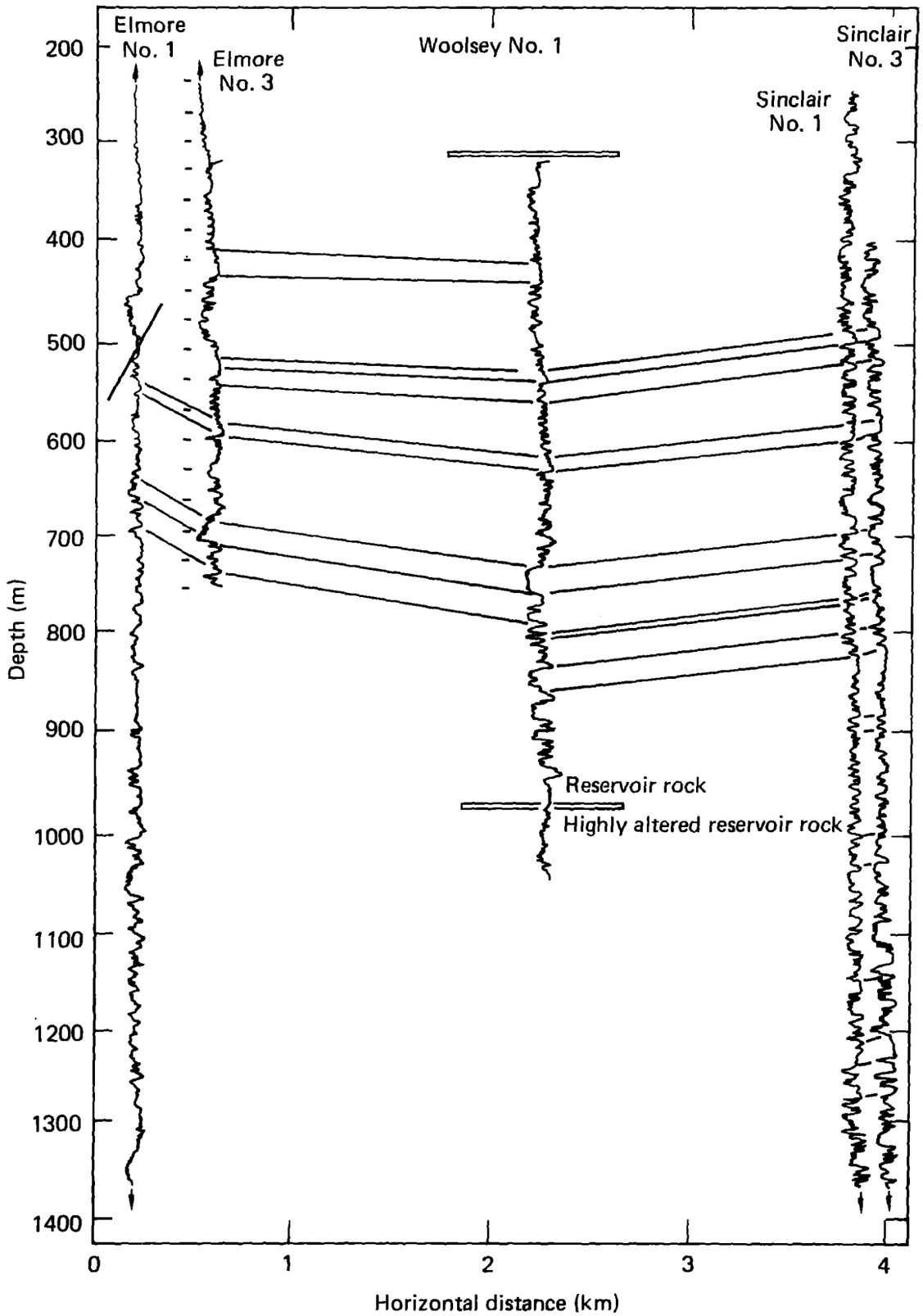

Younker--Fig. 6

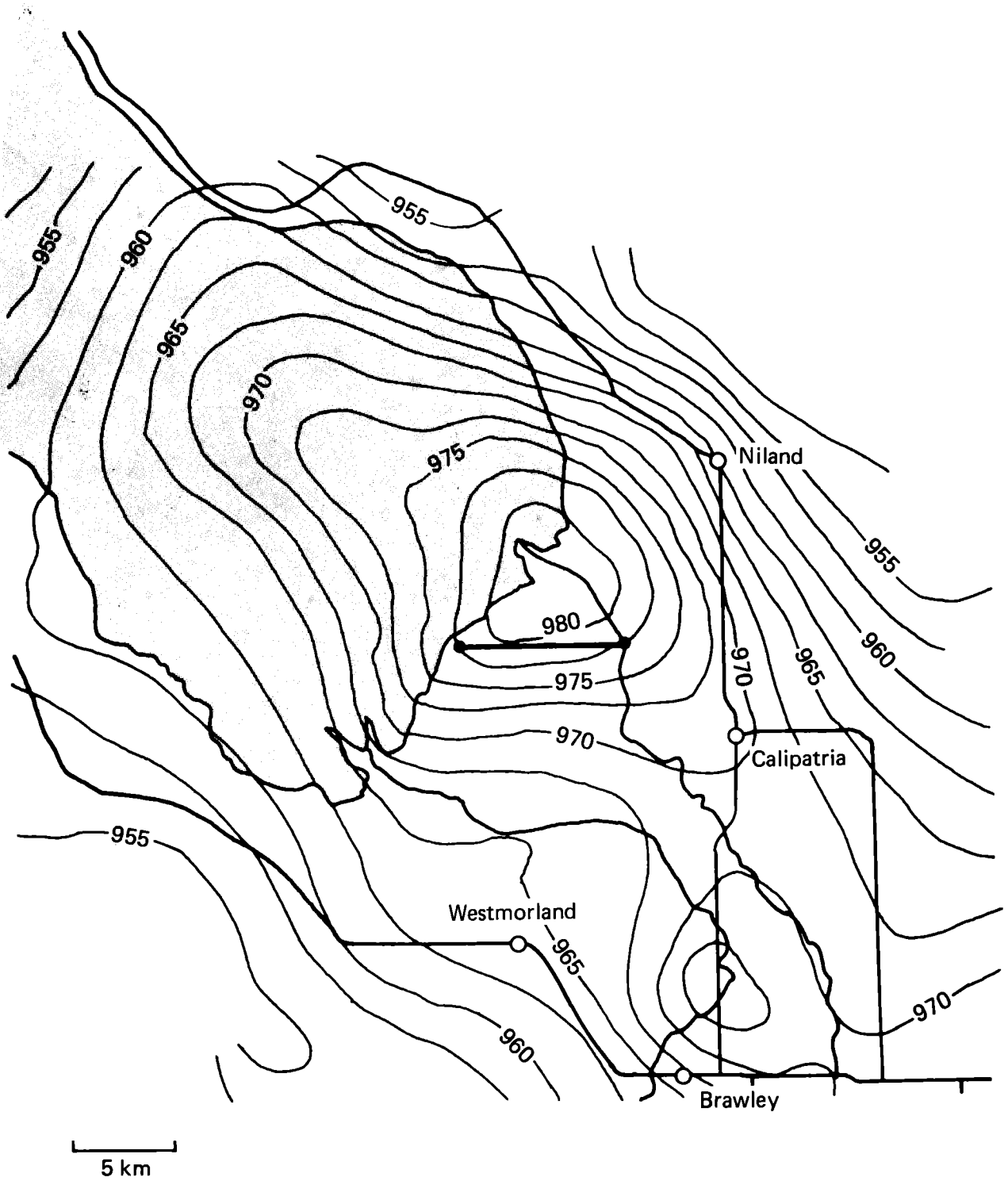

Younker--Fig. 7

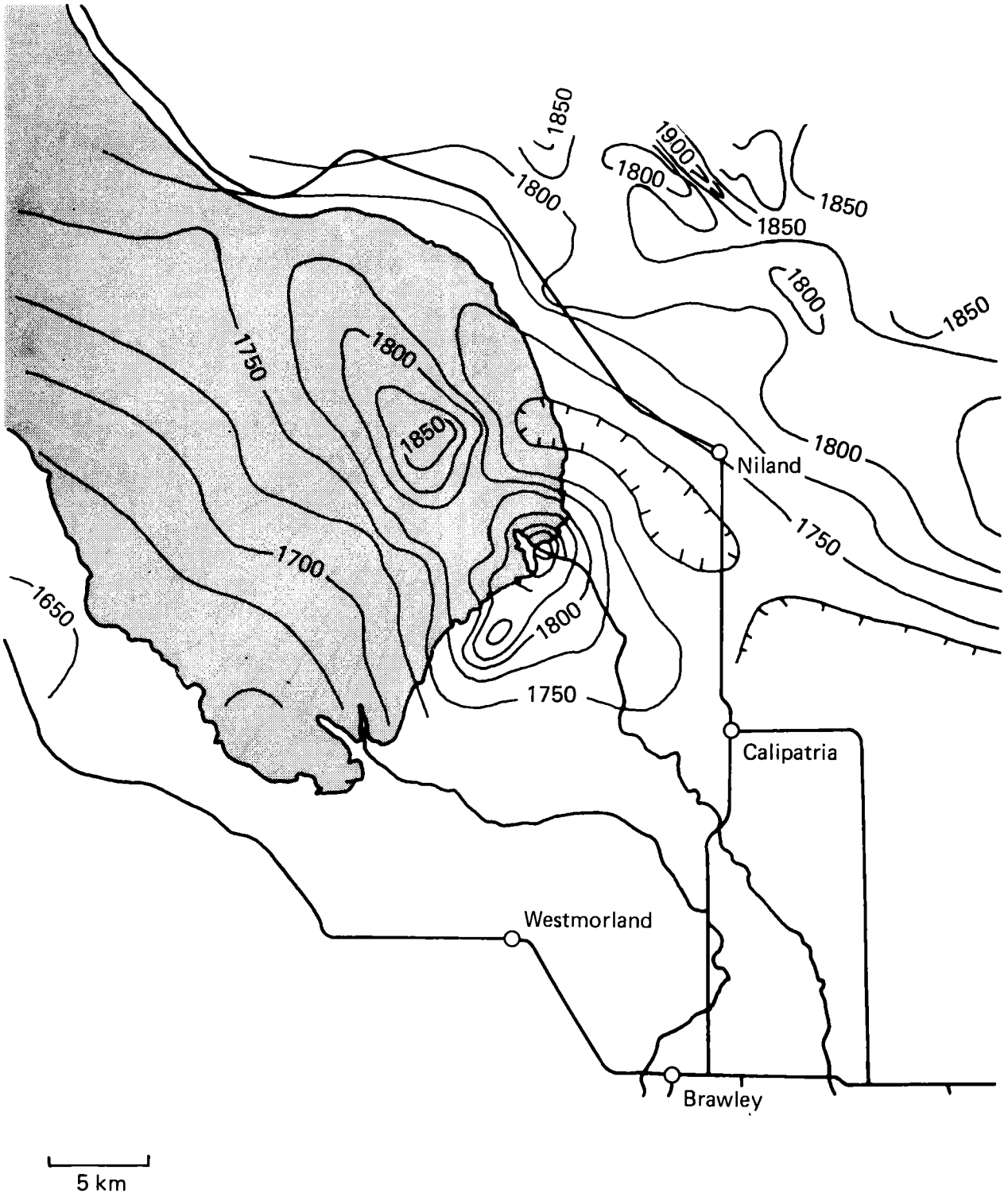

Younker--Fig. 8

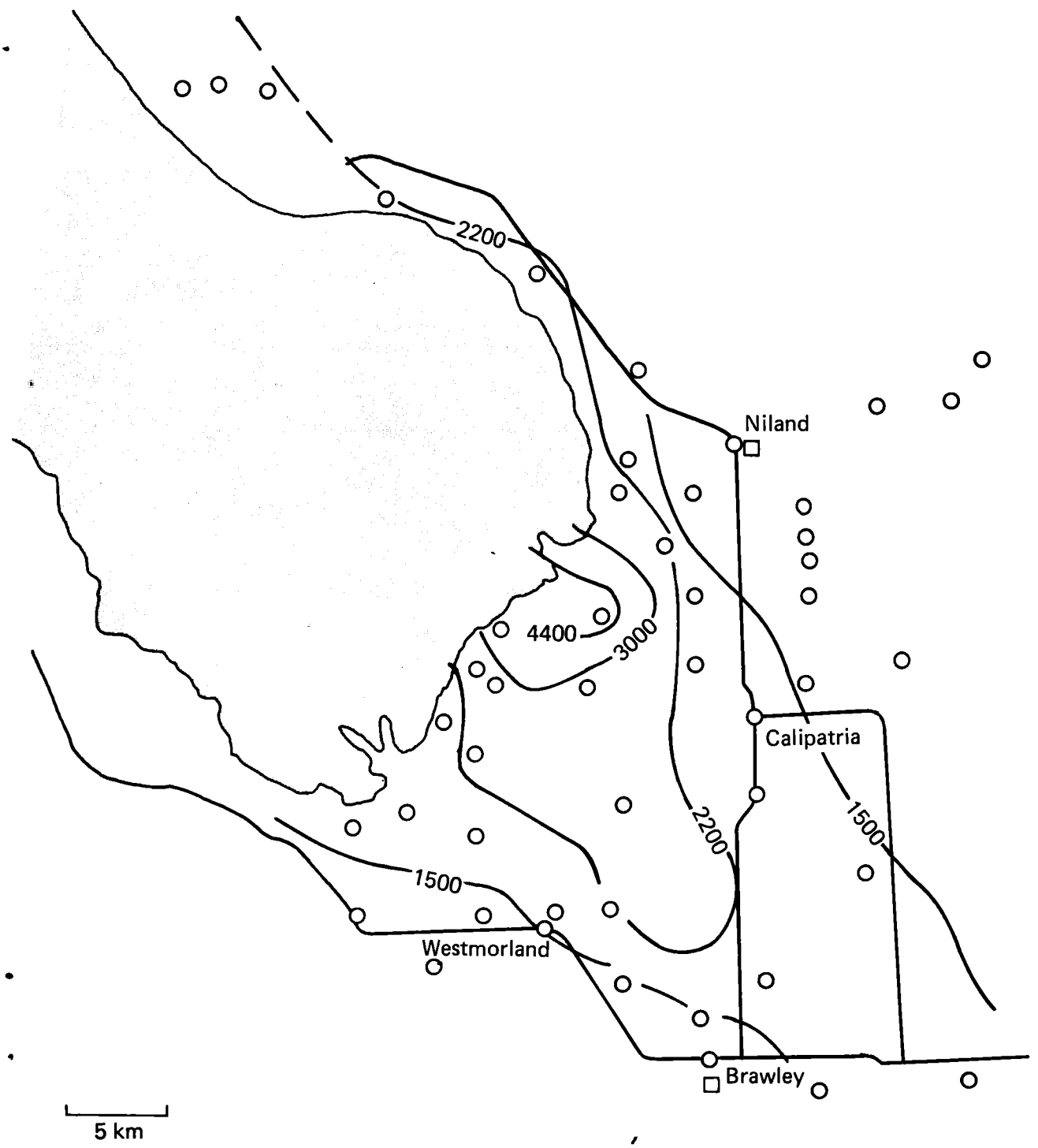

Younker--Fig. 9

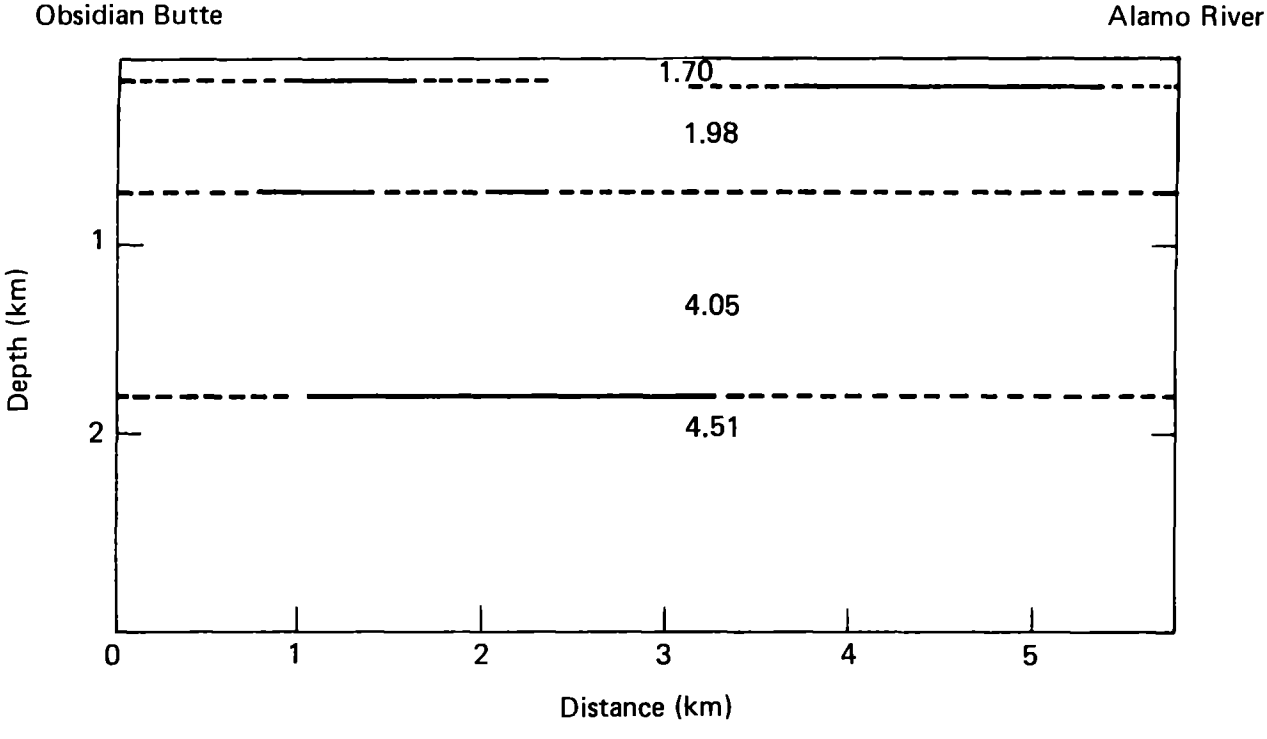

Younker--Fig. 10

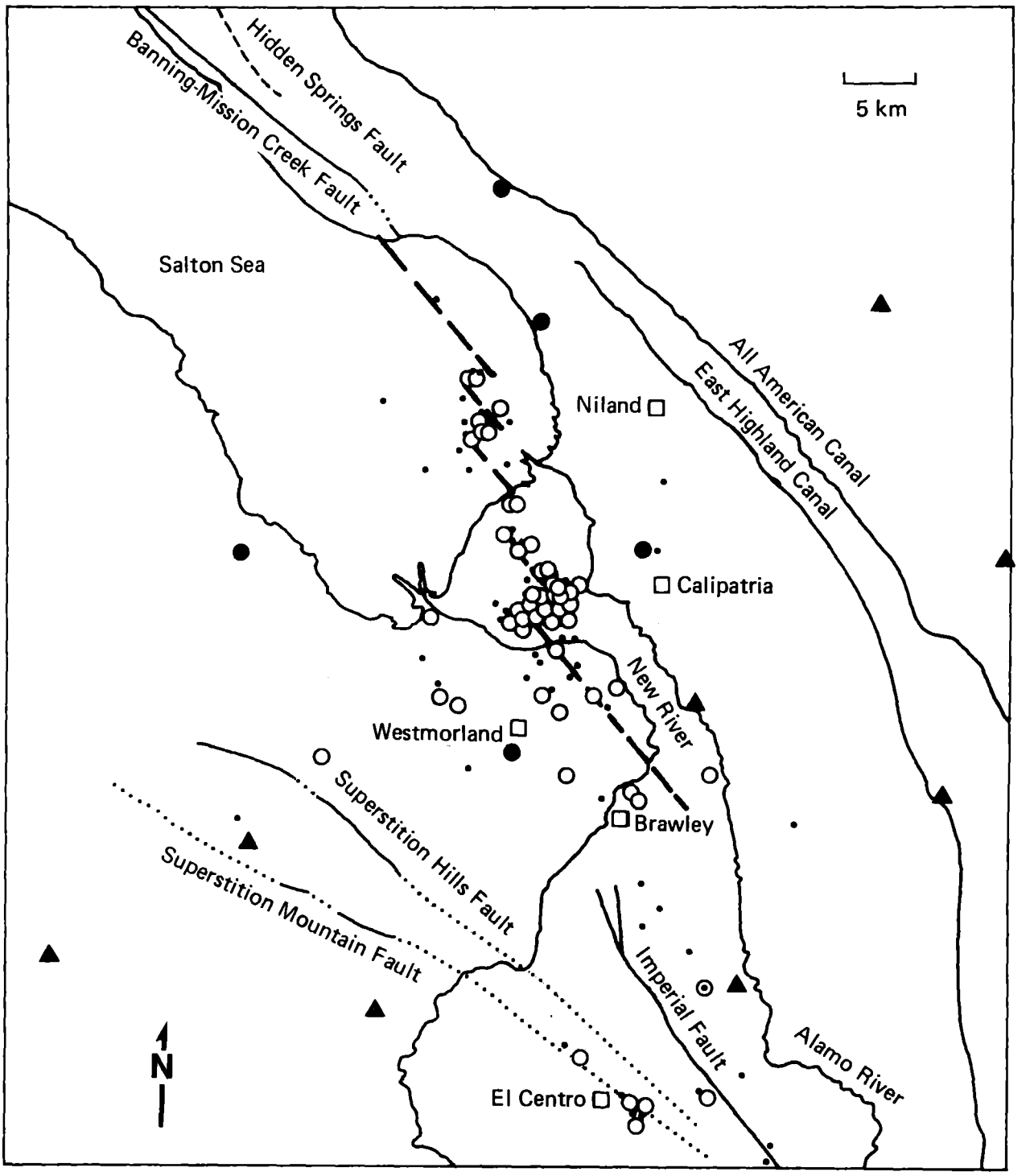

Younker-- Fig. 11

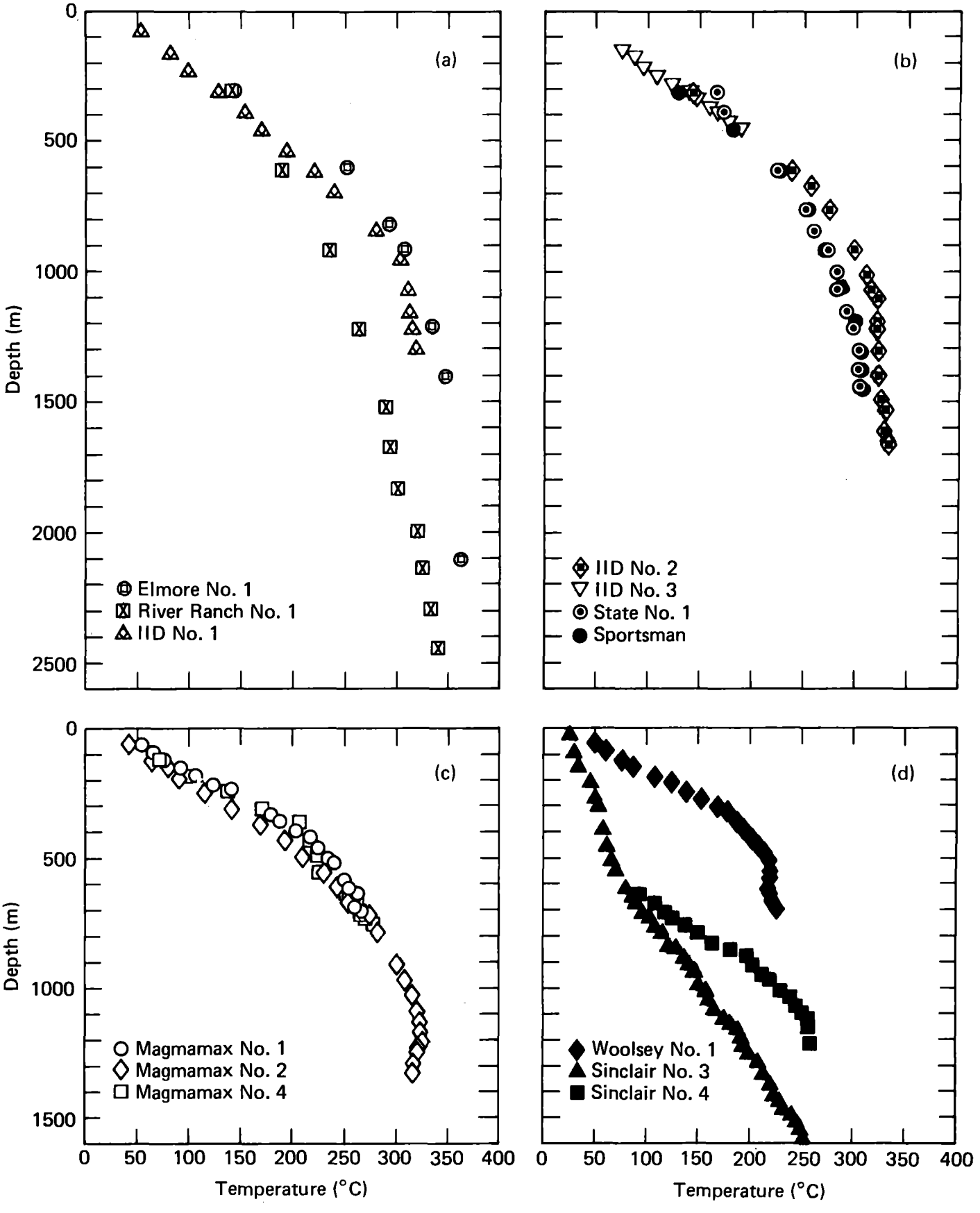
(a)
(b)
(c)
(d)
Depth (m)
Temperature (°C)
Elmore No. 1
River Ranch No. 1
IID No. 1
IID No. 2
IID No. 3
State No. 1
Sportsman
Magmamax No. 1
Magmamax No. 2
Magmamax No. 4
Woolsey No. 1
Sinclair No. 3
Sinclair No. 4

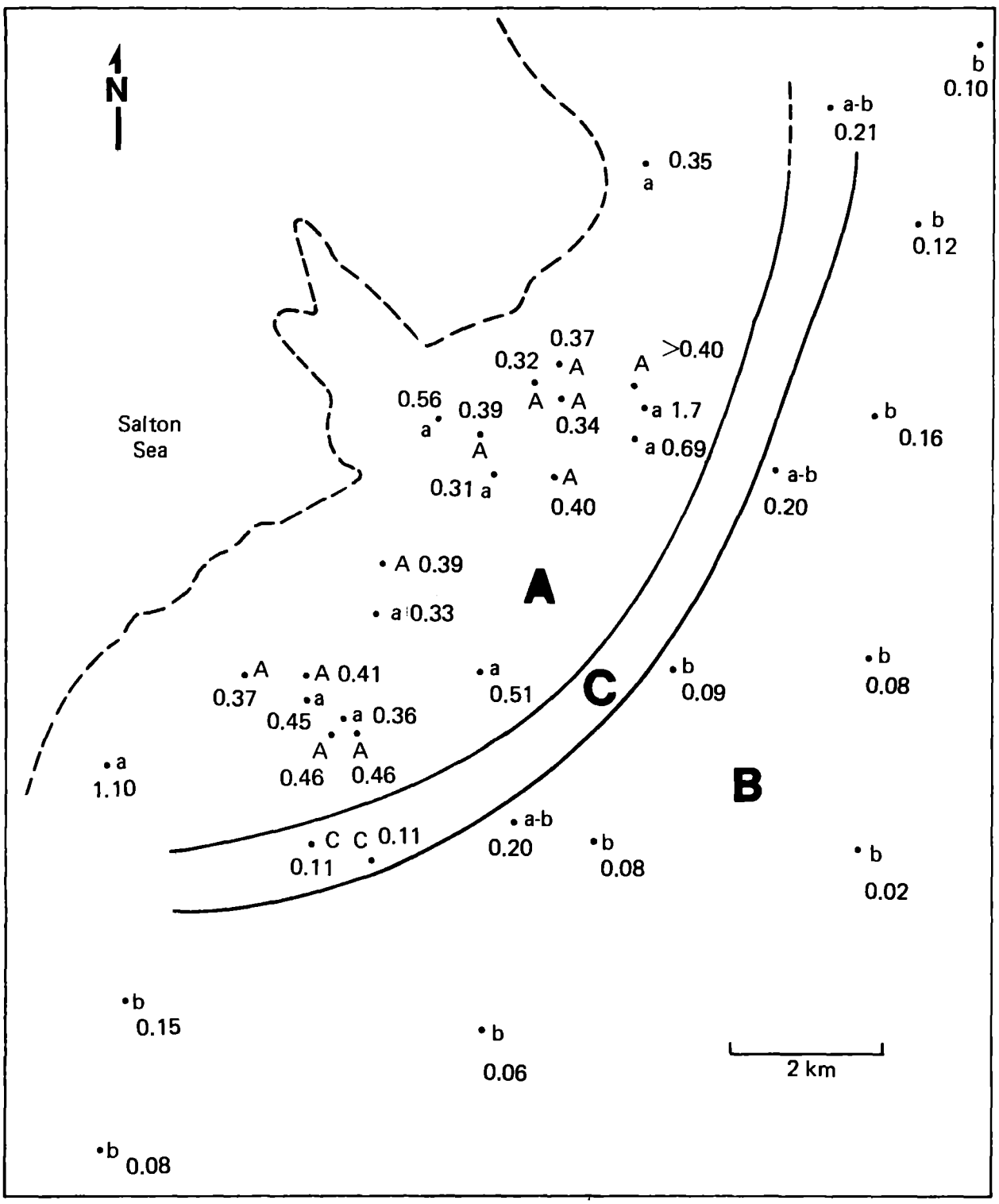

Younker--Fig. 13

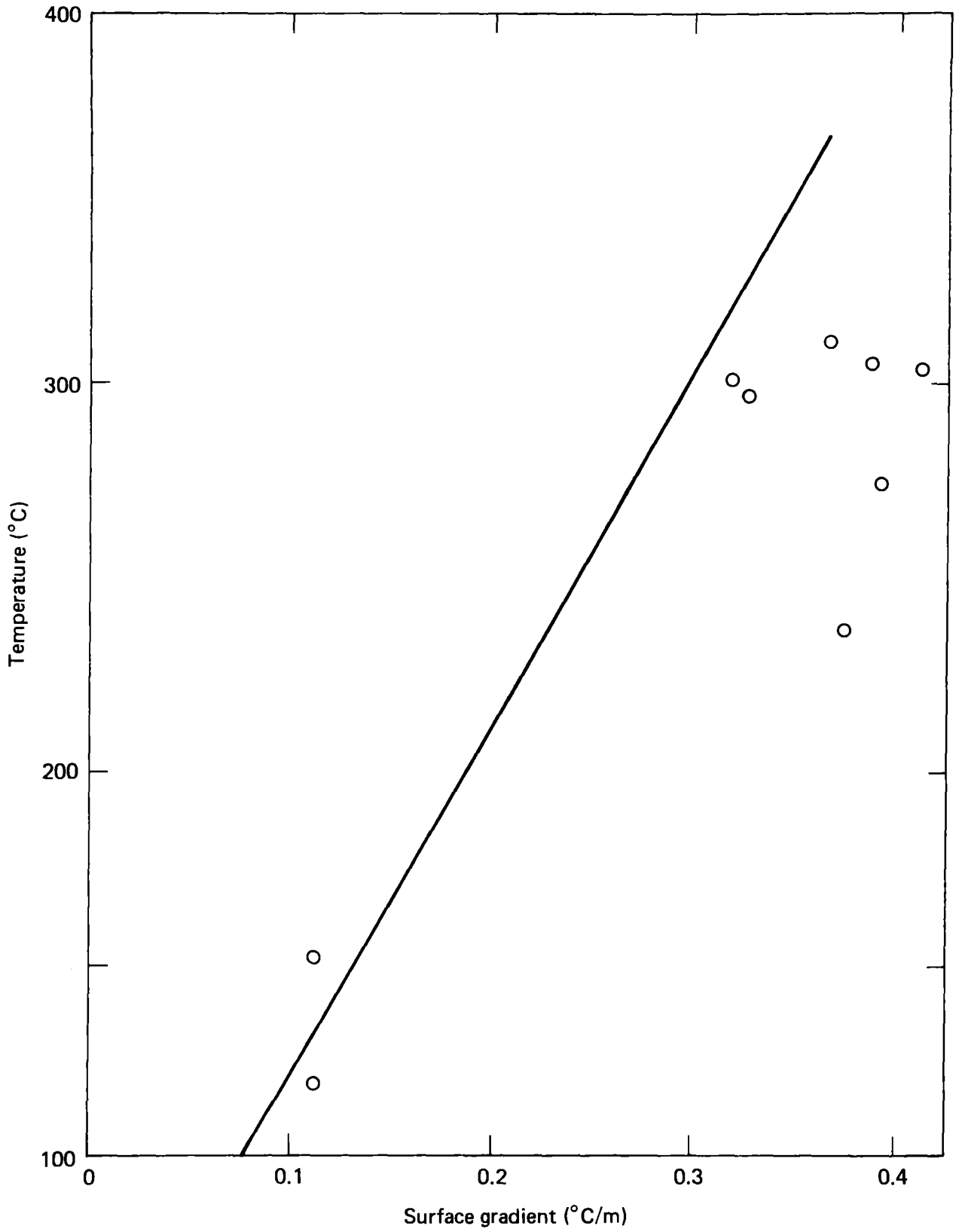

Younker--Fig. 14

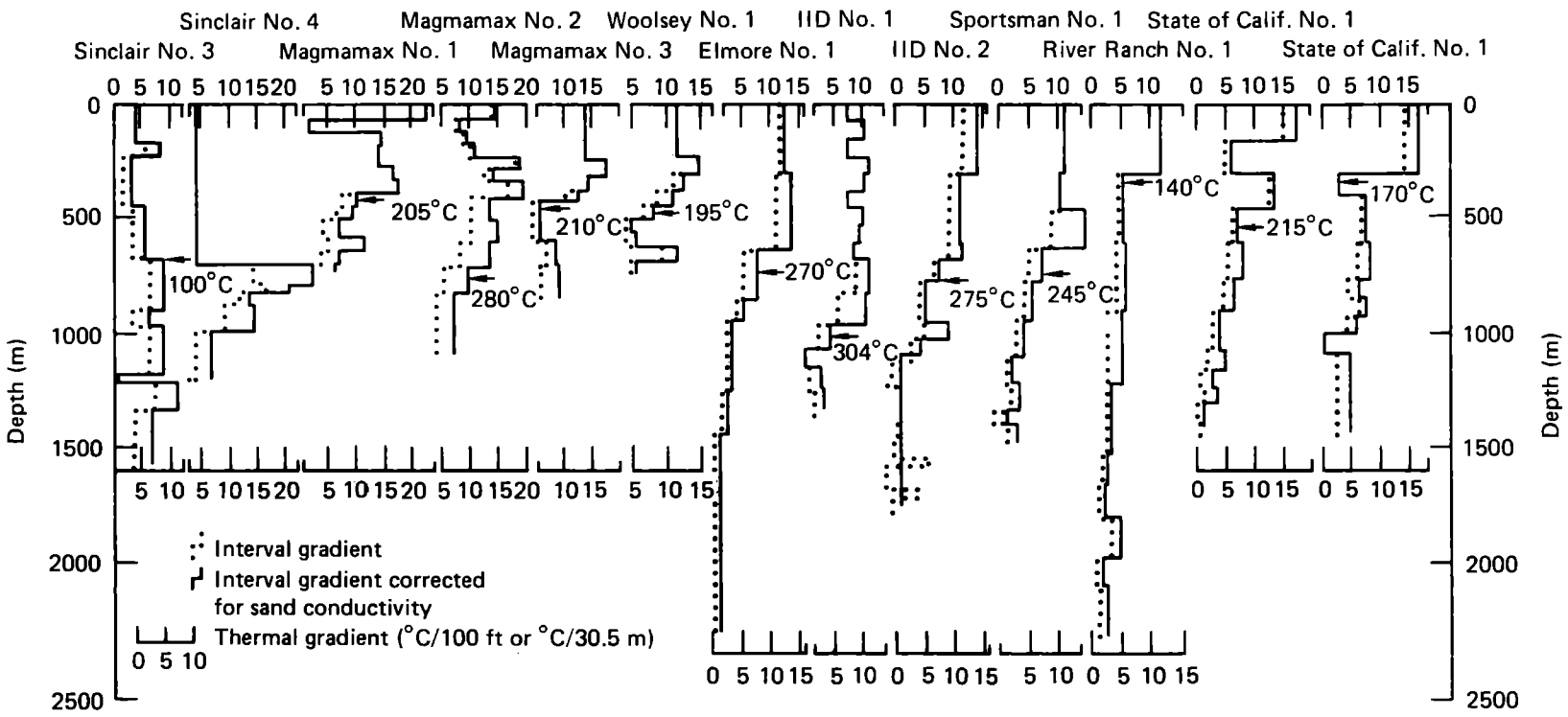

Younker--Fig. 15

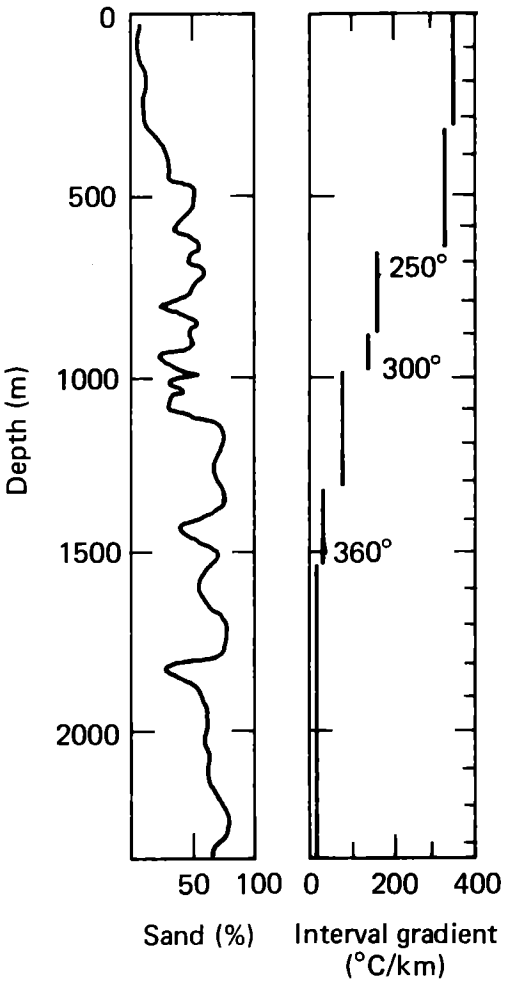

Younker--Fig. 16

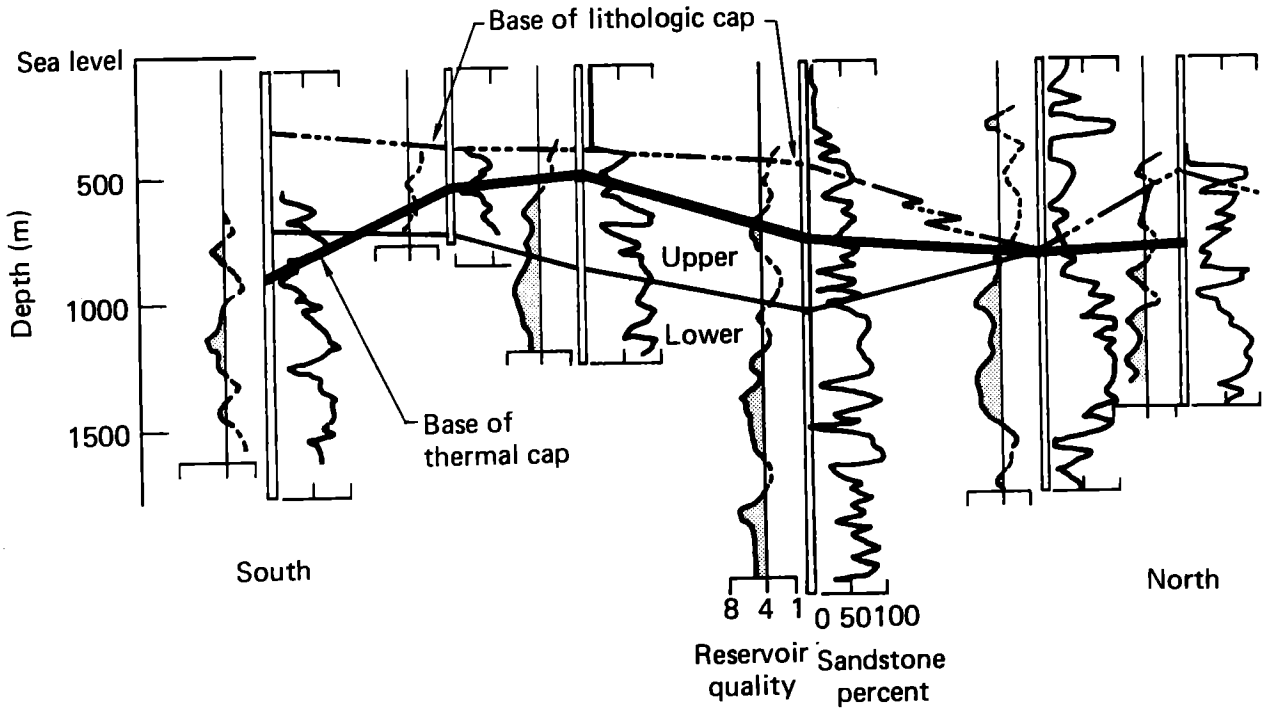

Younker--Fig. 17

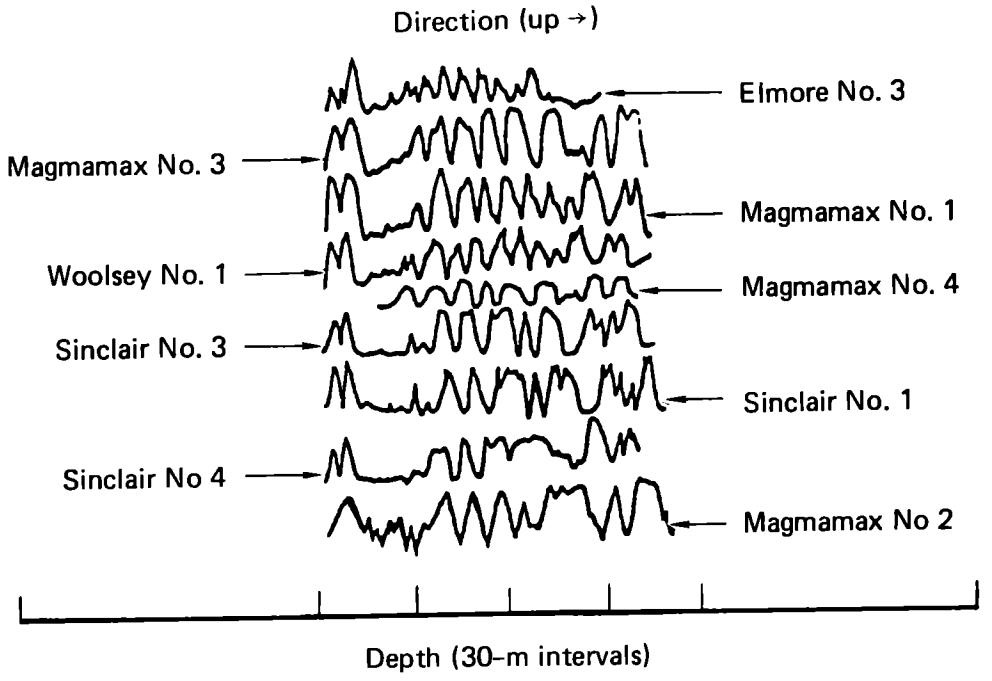

Younker--Fig. 18

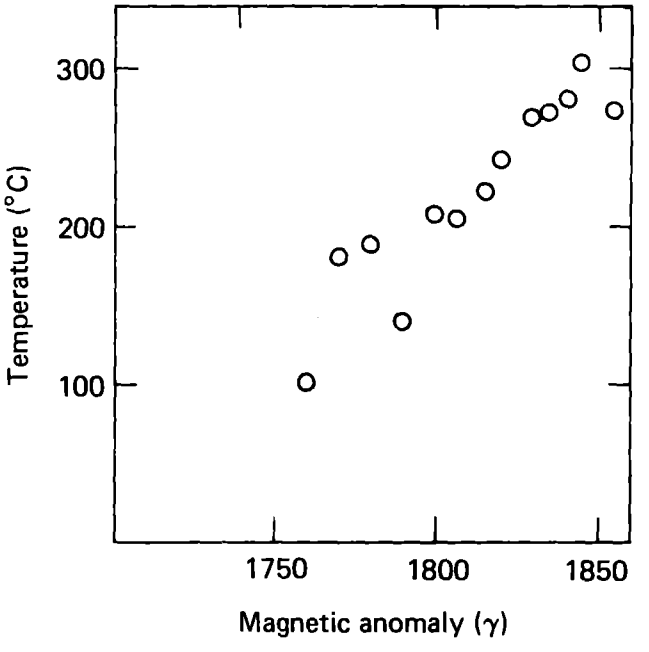

Younker--Fig. 19

Unit	Lithology	Heat transfer
Cap rock	Thick unconsolidated silt, sand, gravel, and anhydrite-rich deposits	Heat flow by conduction
Slightly altered reservoir	Shale and sand Small sand units	Enhanced conductivity resulting from presence of sand; still part of thermal cap
	Upper reservoir Shales, siltstone, and sandstone cemented by calcite or silica	Convection within sand units; shales separate region into isolated hydrologic systems
	Major shale break	
Highly altered reservoir	Lower reservoir Reduced permeability results when altered by replacement of calcite with epidote; extensively fractured	Fractures allow more extensive convection patterns
Zone of intrusion	Intrusion of small basaltic dikes and sills into sedimentary section; less than 20% intrusive bodies	Rate of heat release is a function of rate of intrusion

Younker--Fig. 20